

# Strategic Storage Use in a Hydro-Thermal Power System with Carbon Constraints

Sébastien Debia<sup>a</sup>, Pierre-Olivier Pineau<sup>a</sup>, Afzal S. Siddiqui<sup>b,c,d,a,\*</sup>

<sup>a</sup>*Department of Decision Sciences, HEC Montréal, Canada*

<sup>b</sup>*Department of Computer and Systems Sciences, Stockholm University, Sweden*

<sup>c</sup>*Department of Mathematics and Systems Analysis, Aalto University, Finland*

<sup>d</sup>*Department of Statistical Science, University College London, United Kingdom*

---

## Abstract

Several interconnected power systems worldwide have largely thermal and hydro production along with CO<sub>2</sub> cap-and-trade (C&T) systems and variable renewable energy sources (VRES). C&T policies increase VRES generation, and socially optimal storage deployment could integrate VRES output. However, hydro reservoirs may be used strategically due to market power. We investigate these distortions and assess measures for their mitigation via a bottom-up equilibrium model of New York and Québec. In particular, we find evidence that hydro producers shift water between seasons to manipulate electricity prices even under a net-hydro production constraint. Alternative regulation covering net imports as well as net-hydro production limits such *temporal arbitrage* but enables firms with both thermal generation and pumped-hydro storage to exercise *spatial arbitrage*. We demonstrate that these distortions will be exacerbated under more stringent C&T policies because price-taking thermal producers are less able to respond to price signals.

*Keywords:* Electricity markets, Equilibrium modeling, Hydropower, Market power, Carbon policy

---

## 1. Introduction

Pathways to a low-carbon future usually entail electrifying most energy sectors and decarbonizing electricity generation (Steinberg et al., 2017). Output from renewable energy sources will, therefore, have to grow and become a larger share of the generation mix. At the same time, carbon constraints will increasingly be used to incentivize their penetration. The state of New York is illustrative of this by aiming for 70% of the state's electricity to come from renewable sources by 2030 and reducing 100% of the electricity sector's greenhouse gas emissions by 2040 (New York State, 2019), notably by using a cap-and-trade (C&T) market in the power sector to reduce emissions (RGGI, 2019). While capacities of variable renewable energy sources (VRES) such as wind and solar are quickly growing, cf. a 50% increase from 2019 to 2024 (IEA, 2019), power systems will need more flexibility to integrate them (Lund et al., 2015). Large-scale hydropower with reservoirs provides flexibility

---

\*Corresponding author

*Email addresses:* [sebastien.debia@hec.ca](mailto:sebastien.debia@hec.ca) (Sébastien Debia), [pierre-olivier.pineau@hec.ca](mailto:pierre-olivier.pineau@hec.ca) (Pierre-Olivier Pineau), [asiddiq@dsv.su.se](mailto:asiddiq@dsv.su.se) (Afzal S. Siddiqui)

toward this end (Hirth, 2016), but such a storage option in markets with strategic players can create new opportunities for manipulating market prices (Tangerås and Mauritzen, 2018). As there are several such hydro-thermal power systems with carbon constraints worldwide, e.g., California, Italy, Manitoba-Minnesota, New York-Québec, and Nord Pool, our objective is to understand strategic behavior in these contexts by using New York-Québec as our case study in order to inform future energy policy.

The possibility of enhanced leverage by flexible producers has been investigated since the deregulation of the electricity industry. Seminal works include Crampes and Moreaux (2001) and Bushnell (2003) who focused on hydro producers' Cournot behavior. In a stylized two-period duopoly model of a hydro-thermal electricity market, Crampes and Moreaux (2001) prove that Cournot hydro producers have the incentive to use more water during the first, i.e., off-peak, period than under perfect competition in order to enable strategic withholding in the second, i.e., peak, period. Consequently, this intertemporal arbitrage increases (decreases) the electricity price in the peak (off-peak) period vis-à-vis perfect competition and may even result in negative water values. Such a supposition is investigated via a numerical implementation of a Nash-Cournot model for the California and Pacific Northwest hydro-thermal power system by Bushnell (2003). In spite of a regulatory constraint that prohibits "spilling" of water, i.e., hydro producers are required to generate from all of the water allocated to them, strategic producers profit from over-generating during off-peak hours in order to create scarcity and further raise prices during peak hours. Since such Cournot hydro producers would actually benefit from the additional scarcity created by less water allocation, they have negative monthly water values.

Ongoing adoption of VRES capacity has piqued interest in other forms of storage besides hydro reservoirs. Sioshansi (2010) analyzes the many positive welfare impacts of generic storage use via a stylized partial-equilibrium model with perfectly competitive electricity generation. Ownership of storage is shown to be important as it affects the incentives to use it optimally. Examining departures from perfect competition, Sioshansi (2014) finds instances of welfare-reducing storage arising from its strategic use. In a similar vein, Debia et al. (2019) explore carbon pricing's effects on producer behavior in a stylized VRES-thermal power system with storage. In particular, higher storage efficiency enhances welfare but conflicts with the storage owner's profit-maximization objective in some situations, which may be remedied by a carbon tax to align social and private incentives better. Focusing on the storage-investment decision via a Stackelberg leader-follower model, Siddiqui et al. (2019) show that a profit-maximizing merchant investor may actually adopt more storage capacity than a hypothetical welfare-maximizing one if the generation sector is sufficiently competitive.

These aforementioned papers use stylized models of hydro and storage operations with the objective of obtaining general insights to support policy. However, they abstract from certain details of the electricity industry, such as transmission constraints, intermittent VRES output, and unit-commitment restrictions. The engineering literature focuses on these aspects with the intention of devising numerical solutions to large-scale problem instances instead of explicitly deriving economic insights (Aasgård et al., 2014; Finardi and da Silva, 2006). Meanwhile, the papers in this strand of

the literature that explore the potential for market power typically do not conduct welfare analysis or incorporate regulation, e.g., on carbon emissions or water usage, for actual power systems (Flach et al., 2010; Moiseeva and Hesamzadeh, 2018).

Recent work incorporates salient features of power systems with the intention of performing economic analysis of the strategic use of storage and other flexible technologies in actual jurisdictions. For example, Schill and Kemfert (2011) conduct a Nash-Cournot analysis calibrated to German data with various ownership structures to unveil circumstances in which storage operations would actually diminish welfare. Likewise, Virasjoki et al. (2016) show that a transmission-constrained Western European power system with strategic storage operations would facilitate generation withholding by conventional plants. Nasrolahpour et al. (2016) examine how a merchant storage investor could affect market prices through its capacity-sizing decision as a Stackelberg leader in Alberta. The potential for other flexible technologies, such as combined heat and power plants (Virasjoki et al., 2018) and DC interconnections (Debia et al., 2018), to increase the leverage of strategic agents has been demonstrated in game-theoretic models of the Nordic and New York-Québec power systems, respectively. Nevertheless, even in such papers that bridge the physical realism of engineering-type models and the market realism of economic models, either hydro reservoirs or transmission flows are not modeled fully. For example, hydro plants are treated as generic flexible technologies with seasonal availability factors (Bjørndal et al., 2014; Virasjoki et al., 2018), while New York-Québec is represented by three nodes (Debia et al., 2018).

Given the recent empirical evidence for market power in electricity markets due to either hydro storage (Tangerås and Mauritzen, 2018) or arbitrage potential more generally for an integrated producer (Ito and Reguant, 2016), a careful assessment of the role of hydro reservoirs in enabling spatial and temporal arbitrage is warranted. This paper specifically investigates strategic behavior in a hydro-thermal system with reservoirs in the presence of VRES output and a C&T constraint. It builds on the aforementioned literature by exploring welfare impacts of Cournot hydropower generators when they have access to large-scale storage, allowing them to shift generation from one season to another. We use data from the Québec hydropower system and the New York power market (mostly thermal, but with a single owner of large-scale hydropower plants, the New York Power Authority or NYPA) to investigate how (i) market power by producers and strategic use of storage along with (ii) a C&T cap affect welfare outcomes in the region. We devise a realistically calibrated case study incorporating pertinent details of the power system, viz., the network topology based on the “standard grouping” in Figure 1. Our main findings are:

- (i) Hydro producers can exert *temporal arbitrage* by increasing prices in the peak season (winter) and reducing them in the off-peak season (spring).
- (ii) Extending the water-usage regulation in Bushnell (2003) to account for AC network interactions tends to mitigate *temporal arbitrage* but increases the possibility of *spatial arbitrage* instead.
- (iii) A more stringent C&T cap benefits hydro producers and reduces the effectiveness of water regulation but does not change the strategic incentives.

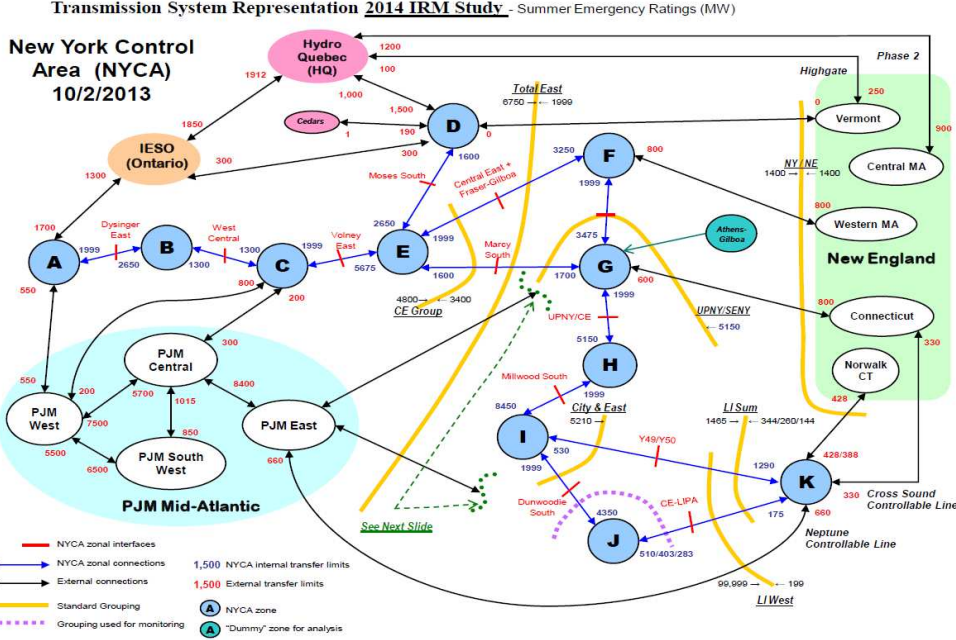


**Figure 1:** Test Network of the New York Control Area (NYSRC, 2012).

The remainder of this paper is structured as follows. Section 2 describes the framework for analysis and specifies the modeling assumptions. In Section 3, we formulate the equilibrium problem and reformulate it to facilitate numerical solutions. Section 4 implements numerical examples for the New York-Québec region, and Section 5 concludes while offering directions for future research. Appendices A and B provide mathematical details about the model and numerical results for a low cap on CO<sub>2</sub> emissions, respectively.

## 2. Research Methodology

We use a Nash-Cournot framework with nodal pricing (Hobbs, 2001), which is standard for analyzing strategic behavior in electricity markets. It is flexible enough to incorporate the texture of the power sector, viz., transmission constraints, ramping restrictions, variability in resource availability, and regulatory requirements, while allowing for interactions between a gross-consumer-surplus-maximizing independent system operator (ISO) and profit-maximizing firms. The scope of our study is a given test year, i.e., a medium-term analysis with fixed capacity, in which variation in VRES output and demand is reflected by representative weeks based on a clustering procedure (Reichenberg et al., 2018). Firms may hold diverse portfolios of generation assets comprising thermal, hydro, and VRES capacity at various nodes, which are connected by transmission lines, and sell power at locational marginal prices (LMPs), which are determined by market clearing in each hour of each representative week. Inverse-demand functions with point elasticities capture consumers' maximum willingness to pay for electricity in each hour at each node. Firms behaving à la Cournot use these inverse-demand functions to determine their profit-maximizing generation levels while taking the decisions of all other firms and the ISO as given, i.e., the Nash-Cournot assumption. Power flows on

AC lines in the network are modeled according to the DC load-flow approximation (Gabriel et al., 2013), whereas DC lines’ power flows are directly controllable and not subject to Kirchhoff’s laws. The ISO controls nodal voltage angles in order to determine the gross-consumer-surplus-maximizing power flows. Finally, we also incorporate regulation on CO<sub>2</sub> emissions (based on the RGGI cap for New York) and water usage (based on Québec’s heritage pool).

Our framework is limited by its abstraction from unit-commitment decisions, the dependency of hydropower production efficiency on the reservoir level, and uncertainty in demand, hydro inflows, and VRES output. Incorporating uncertainty directly would necessitate dynamic decision making, i.e., a closed-loop Cournot model in which each agent updates its strategy after observing periodic realizations of the stochastic parameters. Yet, obtaining a Nash equilibrium in such dynamic games with equilibrium constraints is challenging, especially because the existence and uniqueness of such an equilibrium cannot be guaranteed (Murphy and Smeers, 2005; Singh and Wiszniewska-Matyszek, 2019). Consequently, we use a so-called open-loop Cournot model, which treats all of the decisions as if they were made at once. This assumption simplifies the solution procedure and is justified as long as the industry is reasonably competitive. Even under Cournot behavior, hydro producers’ incentives for temporal arbitrage in a closed-loop model are merely weakened vis-à-vis open-loop Cournot but not eliminated (Crampes and Moreaux, 2001; Debia et al., 2019). Thus, instead of treating uncertainty, we capture temporal variations in relevant parameters by using a cluster of representative weeks.

As for unit-commitment decisions and reservoir-dependent hydropower production efficiencies, they introduce non-convexities that are challenging to resolve in Nash-Cournot models. For example, Ramos et al. (1998) use side constraints in order to reflect strategic behavior such that marginal revenue is greater than or equal to marginal cost only when the unit is committed. However, as Hobbs (2001) mentions, such constraints could be cumbersome to include in multi-period models. Finally, we do not use water values because we assume a medium-term horizon with regulated water usage, cf. Québec’s heritage pool (Hydro-Québec, 2019a). Hence, in spite of these simplifications, our open-loop Cournot model captures the spatial and temporal texture of a hydro-dominated electricity market and is calibrated to reflect the seasonal price variations that underpin strategic decision making (see Section 4.3).

### 3. Problem Formulation

The nomenclature is given in Section 3.1. We then present the problem for each agent in Sections 3.2 and 3.3, while the treatment of regulation follows in Section 3.4.

#### 3.1. Nomenclature

##### *Indices and Sets*

$i \in \mathcal{I}$ : Firms

$\mathcal{I}_{n,w}$ : Firms owning hydro unit  $w$  at node  $n$

$\ell \in \mathcal{L}$ : Transmission lines

$\mathcal{L}^{AC} \subset \mathcal{L}$ : AC transmission lines  
 $\mathcal{L}^{DC} \subset \mathcal{L}$ : DC transmission lines  
 $\mathcal{L}_n^+, \mathcal{L}_n^-$ : Transmission lines starting/ending at node  $n$   
 $n \in \mathcal{N}$ : Nodes  
 $\mathcal{N}_{i,w}$ : Nodes containing hydro unit  $w$  belonging to firm  $i$   
 $n^{AC} \in \mathcal{N}^{AC} \subset \mathcal{N}$ : Nodes connected to AC lines  
 $n^{DC} \in \mathcal{N}^{DC} \subset \mathcal{N}$ : Nodes connected only to DC lines<sup>1</sup>  
 $n_\ell^+, n_\ell^-$ : Node index for starting/ending node of line  $\ell$   
 $t \in \mathcal{T}$ : Hourly time periods  
 $u \in \mathcal{U}$ : Conventional generation unit  
 $\mathcal{U}_{i,n}$ : Conventional generation units located at node  $n$  owned by firm  $i$   
 $w \in \mathcal{W}$ : Hydro units  
 $\mathcal{W}_{i,n}$ : Hydro units located at node  $n$  owned by firm  $i$   
 $\mathcal{A}(w)$ : Immediate ancestors of hydro unit  $w$   
 $\mathcal{C}(w)$ : Immediate children of hydro unit  $w$   
 $\mathcal{D}(w)$ : All descendants of hydro unit  $w$   
 $\Omega^{\text{ISO}}$ : Decision variables of the ISO  
 $\Omega^i$ : Decision variables of firm  $i$   
 $\Omega$ : Decision variables of QP

### Parameters

$A_{n,t}$ : Vertical intercept of inverse demand at node  $n$  in period  $t$  (\$/MWh)  
 $B_\ell$ : Susceptance of line  $\ell$  (S)  
 $C_{i,n,t,u}$ : Operating cost of conventional generation unit  $u$  belonging to firm  $i$  at node  $n$  in period  $t$  (\$/MWh)  
 $E_{i,n,u}$ : CO<sub>2</sub> emission rate of conventional generation unit  $u$  belonging to firm  $i$  at node  $n$  (t/MWh)  
 $\bar{E}$ : Cap on CO<sub>2</sub> emissions (t)  
 $F_{i,n,w}$ : Efficiency of pumped storage of hydro unit  $w$  at node  $n$  belonging to firm  $i$  (MWh/m<sup>3</sup>)  
 $G_{i,n,t,u}$ : Maximum output of conventional generation unit  $u$  belonging to firm  $i$  at node  $n$  in period  $t$  (MWh)  
 $\bar{G}_{i,n,t,u}, \underline{G}_{i,n,t,u}$ : Maximum/minimum ramp rate per time period of conventional generation unit  $u$  belonging to firm  $i$  at node  $n$  in period  $t$  (MWh)  
 $H_i$ : Water volume allocated to firm  $i$  over entire horizon (%)  
 $I_{i,n,t,w}$ : Natural inflow to hydro unit  $w$  belonging to firm  $i$  at node  $n$  in period  $t$  (m<sup>3</sup>)  
 $K_\ell$ : Maximum energy flow on line  $\ell$  (MWh)  
 $P_{i,n,w}$ : Efficiency of hydro unit  $w$  at node  $n$  belonging to firm  $i$  (MWh/m<sup>3</sup>)  
 $\bar{P}_{i,n,w} \left( \equiv P_{i,n,w} + \sum_{w' \in \mathcal{D}(w)} P_{i,n,w'} \right)$ : Aggregated productivity of water in reservoir  $w$  at node  $n$  belonging to firm  $i$  (MWh/m<sup>3</sup>)

---

<sup>1</sup>Note that  $\mathcal{L}^{AC} \cup \mathcal{L}^{DC} = \mathcal{L}$ ,  $\mathcal{L}^{AC} \cap \mathcal{L}^{DC} = \emptyset$ ,  $\mathcal{N}^{AC} \cup \mathcal{N}^{DC} = \mathcal{N}$ .

$R_{i,n,t}$ : VRES output belonging to firm  $i$  at node  $n$  in period  $t$  (MWh)

$\bar{R}_{i,n}$ : Regulation for firm  $i$ 's hydro production at node  $n$  (MWh)

$V$ : Scaling factor for transmission flows (–)

$X_{i,n,w}^0$ : Initial volume of water in reservoir of hydro unit  $w$  belonging to firm  $i$  at node  $n$  ( $\text{m}^3$ )

$\bar{X}_{n,i,w}, \underline{X}_{n,i,w}$ : Maximum/minimum volume of water in reservoir of hydro unit  $w$  at node  $n$  belonging to firm  $i$  ( $\text{m}^3$ )

$Y_{i,n,w}$ : Maximum energy production from hydro unit  $w$  at node  $n$  belonging to firm  $i$  (MWh)

$Z_{n,t}$ : Slope of inverse demand at node  $n$  in period  $t$  ( $\$/\text{MWh}^2$ )

### Primal Variables

$c_{n,t}$ : Energy consumed at node  $n$  in period  $t$  (MWh)

$f_{\ell,t}$ : Energy transferred on line  $\ell$  in period  $t$  (MWh)

$g_{i,n,t,u}$ : Energy produced by conventional generation unit  $u$  in period  $t$  at node  $n$  belonging to firm  $i$  (MWh)

$q_{i,n,t}$ : Net generation at node  $n$  and period  $t$  by firm  $i$  (MWh)

$s_{i,n,t,w}$  ( $= 0$  if  $\mathcal{C}(w) = \emptyset$ ): Volume of water pumped to storage at hydro unit  $w$  at node  $n$  in period  $t$  belonging to firm  $i$  ( $\text{m}^3$ )

$v_{n,t}$ : Voltage angle at node  $n$  in period  $t$  (rad)

$x_{i,n,t,w}$ : Volume of water stored in reservoir of hydro unit  $w$  at node  $n$  at the end of period  $t$  belonging to firm  $i$  ( $\text{m}^3$ )

$y_{i,n,t,w}$ : Volume of water turbined by hydro unit  $w$  at node  $n$  in period  $t$  belonging to firm  $i$  ( $\text{m}^3$ )

$z_{i,n,t,w}$ : Volume of water spilled by hydro unit  $w$  at node  $n$  in period  $t$  belonging to firm  $i$  ( $\text{m}^3$ )

### Dual Variables

$\alpha_{i,n,t,w}$ : Shadow price of hydro capacity for unit  $w$  at node  $n$  in period  $t$  belonging to firm  $i$  ( $\$/\text{m}^3$ )

$\beta_{i,n,t,u}$ : Shadow price of maximum conventional capacity for unit  $u$  in period  $t$  at node  $n$  belonging to firm  $i$  ( $\$/\text{MWh}$ )

$\bar{\beta}_{i,n,t,u}/\underline{\beta}_{i,n,t,u}$ : Shadow price of maximum/minimum conventional ramping capacity for unit  $u$  in period  $t$  at node  $n$  belonging to firm  $i$  ( $\$/\text{MWh}$ )

$\gamma_{i,n}$ : Shadow price of water capacity allocated to firm  $i$  at node  $n$  ( $\$/\text{m}^3$ )

$\delta_{i,n,t,w}$ : Shadow price of hydro turbined capacity for unit  $w$  at node  $n$  in period  $t$  belonging to firm  $i$  ( $\$/\text{m}^3$ )

$\bar{\kappa}_{n,t}/\underline{\kappa}_{n,t}$ : Shadow price of maximum/minimum voltage angle at node  $n$  in period  $t$  ( $\$/\text{rad}$ )

$\lambda_{n,t}$ : Shadow price of energy balance at node  $n$  in period  $t$  ( $\$/\text{MWh}$ )

$\bar{\mu}_{\ell,t}/\underline{\mu}_{\ell,t}$ : Shadow price of maximum/minimum capacity on line  $\ell$  in period  $t$  ( $\$/\text{MWh}$ )

$\xi_{i,n,t}$ : Shadow price of energy balance for firm  $i$  at node  $n$  in period  $t$  ( $\$/\text{MWh}$ )

$\rho$ : Price of  $\text{CO}_2$  emission permit ( $\$/\text{t}$ )

$\psi_{\ell,t}$  ( $\equiv 0$  if  $\ell \in \mathcal{L}^{DC}$ ): Shadow price of energy flow constraint on line  $\ell$  in period  $t$  ( $\$/\text{MWh}$ )

$\bar{\omega}_{i,n,t,w}/\underline{\omega}_{i,n,t,w}$ : Shadow price of maximum/minimum reservoir capacity for unit  $w$  at node  $n$  in period  $t$  belonging to firm  $i$  ( $\$/\text{m}^3$ )

### 3.2. ISO

The ISO maximizes gross consumer surplus (1) while meeting network constraints and taking the decisions of the firms as given (Gabriel and Leuthold, 2010). Nodal consumption,  $c_{n,t}$ , is implicitly defined by power flows,  $f_{\ell,t}$ , which are, in turn, implicitly defined by voltage angles,  $v_{n,t}$ , in an AC network.<sup>2</sup> We model both AC and DC lines via a DC load-flow linearization with DC links (Bjørndal et al., 2014).

$$\max_{\Omega^{\text{ISO}}} \sum_{n \in \mathcal{N}} \sum_{t \in \mathcal{T}} \left[ A_{n,t} c_{n,t} - \frac{1}{2} Z_{n,t} c_{n,t}^2 \right] \quad (1)$$

$$\text{s.t. } c_{n,t} - \sum_{i \in \mathcal{I}} q_{i,n,t} - V \left( \sum_{\ell \in \mathcal{L}_n^-} f_{\ell,t} - \sum_{\ell \in \mathcal{L}_n^+} f_{\ell,t} \right) = 0 : \lambda_{n,t}, \forall n, t \quad (2)$$

$$f_{\ell,t} - B_{\ell} \left( v_{n_{\ell}^+, t} - v_{n_{\ell}^-, t} \right) = 0 : \psi_{\ell,t}, \forall \ell, \ell \in \mathcal{L}^{\text{AC}} \quad (3)$$

$$\underline{\mu}_{\ell,t} : -K_{\ell} \leq V f_{\ell,t} \leq K_{\ell} : \bar{\mu}_{\ell,t}, \forall \ell, t \quad (4)$$

$$\underline{\kappa}_{n,t} : -\pi \leq v_{n,t} \leq \pi : \bar{\kappa}_{n,t}, \forall n \in \mathcal{N}^{\text{AC}}, t \quad (5)$$

Here,  $\Omega^{\text{ISO}} \equiv \{c_{n,t} \geq 0, f_{\ell,t}, v_{n,t}\}$  is the set of the ISO's decision variables. Constraint (2) ensures that nodal net production,  $\sum_{i \in \mathcal{I}} q_{i,n,t}$ , and net imports,  $V \left( \sum_{\ell \in \mathcal{L}_n^-} f_{\ell,t} - \sum_{\ell \in \mathcal{L}_n^+} f_{\ell,t} \right)$ , match consumption,  $c_{n,t}$ .<sup>3</sup> Constraint (3) is the loop-flow constraint for AC lines using a DC load-flow linearization based on Kirchhoff's current law in a circuit, i.e., the flow on an AC line connecting two nodes is proportional to the difference in the voltage angles between the two nodes and dependent on the line's susceptance,  $B_{\ell}$ . Constraints (4) and (5) ensure that the maximum capacities of transmission lines and limits on voltage angles are not exceeded, respectively.

### 3.3. Firm $i \in \mathcal{I}$

Each firm takes the ISO's decisions,  $\Omega^{\text{ISO}}$ , as given along with those of other firms in order to maximize its profit (6), which consists of revenue from sales minus the cost of conventional generation. The revenue term takes into account the Cournot behavior of firm  $i$  by stating the nodal price in terms of consumption, i.e., the price at node  $n$  during period  $t$  is  $A_{n,t} - Z_{n,t} \left( \sum_{i' \in \mathcal{I}} q_{i',n,t} + V \left( \sum_{\ell \in \mathcal{L}_n^-} f_{\ell,t} - \sum_{\ell \in \mathcal{L}_n^+} f_{\ell,t} \right) \right)$ . Net production,  $q_{i,n,t}$ , by firm  $i$  at node  $n$  at time  $t$  is explicitly represented by (7), which takes VRES output as given according to its available capacity,  $R_{i,n,t}$ . Controllable generation includes conventional output,  $\sum_{u \in \mathcal{U}_{i,n}} g_{i,n,t,u}$ , and net-hydro production,  $\sum_{w \in \mathcal{W}_{i,n}} P_{i,n,w} y_{i,n,t,w} - \sum_{w \in \mathcal{W}_{i,n}} F_{i,n,w} s_{i,n,t,w}$ . The associated dual variable,  $\xi_{i,n,t}$ , is the marginal revenue of firm  $i$  at node  $n$  during period  $t$ . Constraints (8)–(9) reflect the capacity and ramping constraints on conventional generation capacity. Constraints (10) and (11) update the reservoir's water volume and maintain the water level within limits, respectively (Førsund, 2015). In particular, (10) states that the change in reservoir level,  $x_{i,n,t,w} - x_{i,n,t-1,w}$ , between periods

<sup>2</sup>The ISO explicitly determines the flow on DC lines.

<sup>3</sup>The scalar  $V$  is used to scale the transmission flows in order to improve computational solutions to problem instances. The lower-case Greek letters adjacent to the constraints are the associated dual variables.



$t - 1$  and  $t$  equals the natural inflow,  $I_{i,n,t,w}$ , plus the water released by its immediately upstream reservoirs,  $\sum_{w' \in \mathcal{A}(w)} (y_{i,n,t-1,w'} + z_{i,n,t-1,w'} - s_{i,n,t,w'})$ , minus the net water used by the reservoir,  $y_{i,n,t,w} + z_{i,n,t,w} - s_{i,n,t-1,w}$ . Constraint (12) is the capacity limit on hydro production. All decision variables are non-negative except for  $q_{i,n,t}$ .

$$\max_{\Omega^i} \sum_{n \in \mathcal{N}} \sum_{t \in \mathcal{T}} \left\{ q_{i,n,t} \left[ A_{n,t} - Z_{n,t} \left( \sum_{i' \in \mathcal{I}} q_{i',n,t} + V \left( \sum_{\ell \in \mathcal{L}_n^-} f_{\ell,t} - \sum_{\ell \in \mathcal{L}_n^+} f_{\ell,t} \right) \right) \right] - \sum_{u \in \mathcal{U}_{i,n}} C_{i,n,t,u} g_{i,n,t,u} \right\} \quad (6)$$

$$\text{s.t. } q_{i,n,t} - \left[ \sum_{u \in \mathcal{U}_{i,n}} g_{i,n,t,u} + R_{i,n,t} + \sum_{w \in \mathcal{W}_{i,n}} P_{i,n,w} y_{i,n,t,w} - \sum_{w \in \mathcal{W}_{i,n}} F_{i,n,w} s_{i,n,t,w} \right] = 0 : \xi_{i,n,t}, \forall n, t \quad (7)$$

$$g_{i,n,t,u} \leq G_{i,n,t,u} : \beta_{i,n,t,u}, \forall n, t, u \in \mathcal{U}_{i,n} \quad (8)$$

$$\underline{\beta}_{i,n,t,u} : \underline{G}_{i,n,t,u} \leq g_{i,n,t,u} - g_{i,n,t-1,u} \leq \overline{G}_{i,n,t,u} : \overline{\beta}_{i,n,t,u}, \forall n, t, u \in \mathcal{U}_{i,n} \quad (9)$$

$$x_{i,n,t,w} - I_{i,n,t,w} - x_{i,n,t-1,w} + (y_{i,n,t,w} + z_{i,n,t,w} - s_{i,n,t-1,w}) - \sum_{w' \in \mathcal{A}(w)} (y_{i,n,t-1,w'} + z_{i,n,t-1,w'} - s_{i,n,t,w'}) = 0 : \alpha_{i,n,t,w}, \forall n, t, w \in \mathcal{W}_{i,n} \quad (10)$$

$$\underline{\omega}_{i,n,t,w} : \underline{X}_{i,n,w} \leq x_{i,n,t,w} \leq \overline{X}_{i,n,w} : \overline{\omega}_{i,n,t,w}, \forall n, t, w \in \mathcal{W}_{i,n} \quad (11)$$

$$P_{i,n,w} y_{i,n,t,w} \leq Y_{i,n,w} : \delta_{i,n,t,w}, \forall n, t, w \in \mathcal{W}_{i,n} \quad (12)$$

Here,  $\Omega^i \equiv \{g_{i,n,t,u} \geq 0, q_{i,n,t}, s_{i,n,t,w} \geq 0, x_{i,n,t,w} \geq 0, y_{i,n,t,w} \geq 0, z_{i,n,t,w} \geq 0\}$  is the set of firm  $i$ 's decision variables.

### 3.4. Regulatory Constraints

The two regulatory constraints in this problem are related to the limits on CO<sub>2</sub> emissions and water usage. Since they are shared among multiple decision makers, this leads to a generalized Nash equilibrium (GNE) problem (Gabriel et al., 2013). We treat this problem using Rosen's normalized equilibrium (Rosen, 1965) with unity weights. The dual variable associated with each regulatory constraint has, therefore, the same value for each player involved. Since these dual variables are the players' marginal valuations of the associated constraints and are set to be equal among the players, each regulatory constraint is interpretable as a market with a unique price. It is, thus, a complete market, which is also competitive since the players take all of the quantities (other than their own) as given (Oggioni et al., 2012).

#### 3.4.1. Carbon Emissions

Constraint (13) limits total system CO<sub>2</sub> emissions to  $\overline{E}$ , which is set exogenously. Using the normalized equilibrium approach, this constraint, despite appearing in each firm's decision problem, is associated with a unique dual variable,  $\rho$ , common to each firm. Hence, (13) is interpretable as

a perfectly competitive C&T market for a public bad (CO<sub>2</sub> emissions) in which the dual variable serves as the opportunity cost of emissions from thermal generation:

$$\bar{E} - \sum_{i \in \mathcal{I}} \sum_{n \in \mathcal{N}} \sum_{t \in \mathcal{T}} \sum_{u \in \mathcal{U}_{i,n}} E_{i,n,u} g_{i,n,t,u} \geq 0 : \rho \quad (13)$$

### 3.4.2. Water Usage

Constraint (14) requires hydro producers to ensure that net-hydro output plus net imports meet a net-annual production potential at each node. As such, both hydro-owning firms and the ISO have to consider the regulation in their optimization problems. Each hydro-owning firm must sell a minimum amount of power,  $\bar{R}_{i,n}$ , at its local node with hydro capacity. The ISO must acquire rights before exporting power from a node with water resource, but it can also sell these rights if it imports at that node, which helps hydro producers to fulfill their obligation. In effect, exports are taxed and imports are subsidized via the dual variable,  $\gamma_{i,n}$ . This formulation is, thus, a floor-and-trade market for a public good (water usage), which is equivalent to a C&T for a public bad:

$$\bar{R}_{i,n} \leq \sum_{t \in \mathcal{T}} \left[ \sum_{w \in \mathcal{W}_{i,n}} (P_{i,n,w} y_{i,n,t,w} - F_{i,n,w} s_{i,n,t,w}) + V \left( \sum_{\ell \in \mathcal{L}_n^-} f_{\ell,t} - \sum_{\ell \in \mathcal{L}_n^+} f_{\ell,t} \right) \right] : \gamma_{i,n}, \forall i, n \in \mathcal{N}_{i,w} \quad (14)$$

By contrast, regulation on water usage in [Bushnell \(2003\)](#) corresponds to (14) without net imports,  $V \left( \sum_{\ell \in \mathcal{L}_n^-} f_{\ell,t} - \sum_{\ell \in \mathcal{L}_n^+} f_{\ell,t} \right)$ . The lower bound,  $\bar{R}_{i,n}$ , specified by an exogenous regulator equals the minimum between the total reserve quantity in the market (such that the price is null) and a share of the total energy available to the hydro producer:<sup>4</sup>

$$\bar{R}_{i,n} \equiv \min \left\{ \sum_{t \in \mathcal{T}} \frac{A_{n,t}}{Z_{n,t}} - \sum_{i' \in \mathcal{I}} R_{i',n,t}, H_i \sum_{w \in \mathcal{W}_{i,n}} \bar{P}_{i,n,w} \left( X_{i,n,w}^0 + \sum_{t \in \mathcal{T}} I_{i,n,t,w} \right) \right\}$$

In the preceding,  $H_i$  specifies the proportion of available water that must be used.

### 3.5. Equilibrium Problem

Using the normalized equilibrium approach of [Rosen \(1965\)](#), each decision maker's problem (including the regulatory constraints) is a convex optimization problem. Thus, each may be replaced by its Karush-Kuhn-Tucker (KKT) conditions, and the GNE problem comprising (1)–(14) may be rendered as a mixed-complementarity problem (MCP). See [Appendix A](#) for the corresponding KKT conditions.

Based on the potential-game approach<sup>5</sup> characterized in [Monderer and Shapley \(1996\)](#) and used in the literature ([Gabriel et al., 2013](#)), we further reformulate the MCP (A-1)–(A-25) as the following

<sup>4</sup>This formulation is to avoid, on average, negative prices at hydro-production nodes.

<sup>5</sup>A potential game consists of summarizing a decentralized decision problem into a single optimization problem with the same optimality (or first-order or stationary) conditions.

single-agent QP by including the so-called “extended cost,”  $-\sum_{i \in \mathcal{I}} Z_{n,t} \frac{q_{i,n,t}^2}{2}$ , in the objective function (15):

$$\begin{aligned} \max_{\Omega} \sum_{n \in \mathcal{N}} \sum_{t \in \mathcal{T}} & \left\{ \left( A_{n,t} c_{n,t} - \frac{1}{2} Z_{n,t} c_{n,t}^2 \right) - \sum_{i \in \mathcal{I}} \left( Z_{n,t} \frac{q_{i,n,t}^2}{2} + \sum_{u \in \mathcal{U}_{i,n}} C_{i,n,t,u} g_{i,n,t,u} \right) \right\} \\ \text{s.t.} & \text{(2) – (5)} \\ & \text{(7) – (12), } \forall i \in \mathcal{I} \\ & \text{(13) – (14)} \end{aligned} \quad (15)$$

where  $\Omega$  comprises the ISO’s decisions,  $\Omega^{\text{ISO}}$ , and all of the firms’ decisions,  $\Omega^i$ ,  $\forall i \in \mathcal{I}$ . The equivalence between the MCP (A-1)-(A-25) and the QP is possible because of the linearity of marginal-cost and inverse-demand functions along with transmission costs that are proportional to network flows (Hashimoto, 1985; Hobbs, 2001). Removing the extended cost,  $-\sum_{i \in \mathcal{I}} Z_{n,t} \frac{q_{i,n,t}^2}{2}$ , from the objective function (15) (likewise, removing the difference between average revenue and marginal revenue,  $Z_{n,t} q_{i,n,t}$ , from (A-10)) renders a perfectly competitive setting because the problem is equivalent to social-welfare maximization.

## 4. Results and Discussion

We use data for New York and Québec to study operations over a test year divided into four seasons.<sup>6</sup>

### 4.1. Data

We simplify the New York Control Area (NYCA) transmission representation (NYSRC, 2012) by treating flows to or from nodes outside of New York and Québec as exogenous parameters netted from consumption (Bushnell and Chen, 2012; Debia et al., 2018). Furthermore, given the “standard grouping” in Figure 1, we treat New York zones A–E and G–I as single nodes in order to obtain the stylized six-node network in Figure 2.<sup>7</sup> Transmission capacities in Table 1 are obtained from NYSRC (2012), whereas AC-line susceptances are calculated based on line lengths and power ratings with a scaling factor of  $V = 500$  (Egerer, 2016).

The conventional, i.e., thermal, generation technologies are combined cycle (CC), gas turbine (GT), nuclear (NU), and steam turbine (ST). There are also the following fuel types (NYISO, 2015): uranium (U), bitumen coal (B), natural gas (G), residual fuel oil (F6), blend of 50% natural gas and 50% residual fuel oil (G6), distilled fuel oil (F2), jet fuel (JF), blend of 50% natural gas and 50% distilled fuel oil (G2), and blend of 50% natural gas and 50% jet fuel (GJ). Since any actual blends were not observable from the data, any 50-50 blends are our assumptions. Consequently, the given

<sup>6</sup>Winter: January-March, Spring: April-June, Summer: July-September, Autumn: October-December.

<sup>7</sup>The directions of the arrows therein indicate the nominally positive direction of power flows, but the actual direction of power flows is determined endogenously, i.e., negative flows are possible.

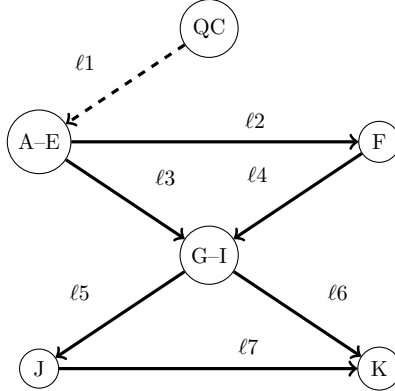


**Figure 2:** Stylized New York-Québec Test Network.

**Table 1:** Line Types, Maximum Thermal Capacities (MW), and Susceptances (S).

Line	Type	$K_\ell$	$B_\ell$
$\ell_1$	DC	1500	–
$\ell_2$	AC	1999	7.5
$\ell_3$	AC	2150	4.7
$\ell_4$	AC	3475	9.4
$\ell_5$	AC	4450	13.4
$\ell_6$	AC	1290	15.2
$\ell_7$	AC	235	14.3

combinations of technologies and fuels yield 11 types of thermal units,<sup>8</sup> which are the  $u \in \mathcal{U}$  used in our formulation. The thermal units’ generation costs are based on 2018 fuel costs and heat rates from [Energy Information Administration \(2018\)](#), while emission rates are calculated as in [Debia et al. \(2018\)](#) with data from [Energy Information Administration \(2018\)](#). The CO<sub>2</sub> cap for New York is 29.2 Mt based on [Bouffard et al. \(2018\)](#). Hourly ramp rates are expressed in terms of fractions of installed capacities,  $G_{i,n,t,u}$ , in Table 2, i.e., as  $\frac{G_{i,n,t,u}}{\bar{G}_{i,n,t,u}}$  ( $= \frac{\bar{G}_{i,n,t,u}}{G_{i,n,t,u}}$ ). The capacity ownership by firm is based on the NYISO Gold Book ([NYISO, 2015](#)) with seasonal adjustments to the indicative installed capacities in Table 3 ([Debia et al., 2018](#)). While operating costs, emission rates, and capacities vary by both technology type and fuel type, the ramp rate depends only on the technology type.<sup>9</sup> Moreover, although operating costs and capacities vary by season, we display the annual average values in Tables 2 and 3, respectively, for sake of brevity. For reference, the underlying average fuel prices by season are given in Figure 3, which exhibit considerable variation for natural gas and capture the high winter electricity prices for New York City (Zone J).

Hydro capacities in the final three columns of Table 4 are partitioned into pumped hydro (PH),

<sup>8</sup>The complete set of thermal units is CC-G, GT-G, GT-F2, GT-JF, GT-G2, GT-GJ, NU-U, ST-B, ST-G, ST-F6, and ST-G6.

<sup>9</sup>ST plants can actually run on coal, natural gas, and fuel oil. The majority of the ST plants in New York use natural gas and fuel oil instead of coal ([NYISO, 2015](#)). Nevertheless, the ramp rates of gas- or oil-fired ST plants are about one-third those of simple-cycle GT plants ([Gonzalez-Salazar et al., 2018](#)).

**Table 2:** Thermal Generation Costs (\$/MWh), Emission Rates (t/MWh), and Ramp Rates (-).

Unit	$C_{i,n,t,u}$	$E_{i,n,u}$	Ramp Rate
CC-G	32.13	0.45	0.5
GT-G	46.95	0.65	1.0
GT-F2	200.61	1.09	1.0
GT-JF	200.47	1.05	1.0
GT-G2	123.78	0.87	1.0
GT-GJ	123.71	0.85	1.0
NU-U	1.89	0.00	0.1
ST-B	35.46	1.03	0.3
ST-G	43.49	0.61	0.3
ST-F6	100.11	0.89	0.3
ST-G6	71.80	0.75	0.3

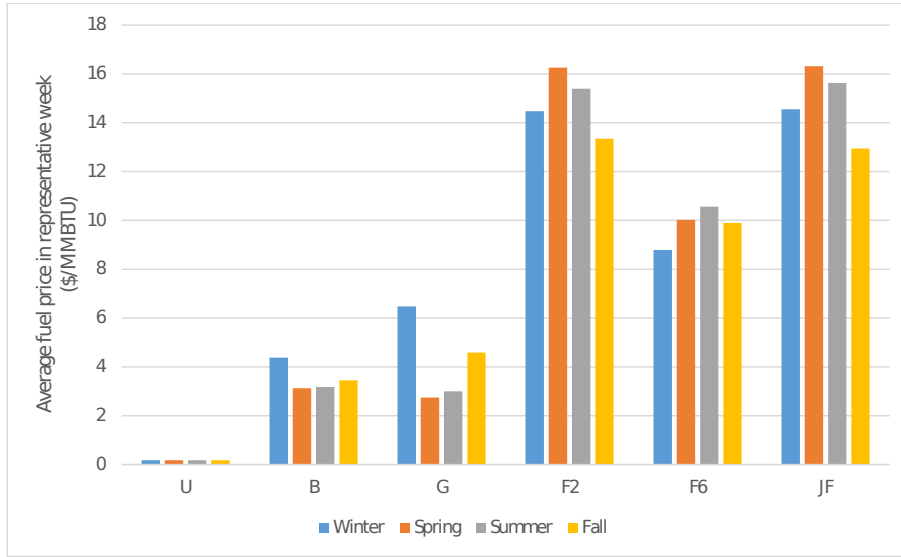


**Figure 3:** Average Fuel Prices in Representative Weeks.

run of river (RR), and reservoir (RS). Data for New York are from [NYISO \(2015\)](#), whereas those for Québec are from [Hydro-Québec \(2019b\)](#).<sup>10</sup> Hydro-production efficiencies are expressed in terms of energy content, i.e.,  $P_{i,n,w} = 1$ , which means that Québec’s RS capacity,  $\bar{X}_{n,i,w}$ , is 176 TWh ([Hydro-Québec, 2019b](#)). In New York, PH efficiency,  $F_{i,n,w} = \frac{1}{0.73}$ , and RS capacity,  $\bar{X}_{n,i,w} = 3 \times Y_{i,n,w}$ , are based on the Blenheim-Gilboa facility’s efficiency and three-hour operating range, respectively ([Wong et al., 2009](#)). Natural inflows,  $I_{i,n,t,w}$ , to RR plants in New York are calibrated to fit seasonal hydro production based on shares of reported NYISO production ([NYISO, 2019](#)). Meanwhile, natural inflows to Québec’s RS plants are assumed to be 85 TWh occurring at the beginning of the year in order to investigate temporal arbitrage as posited by [Bushnell \(2003\)](#). Since Québec’s RR plants are situated immediately downstream of the RS ones and have no natural inflows, they re-use water

<sup>10</sup>HQ: Hydro-Québec, LIPA: Long Island Power Authority, NYPA: New York Power Authority.

**Table 3:** Firms' Conventional ( $G_{i,n,t,u}$ ) Installed Capacities (MW).

$n$	$i$	CC-G	GT-G	GT-F2	GT-JF	GT-G2	GT-GJ	NU-U	ST-B	ST-G	ST-F6	ST-G6
QC	HQ	411										
A-E	Edison	86	2									
	NRG								451		827	829
	Fringe	2333	141					3354	1198			
F	Edison	80										
	Fringe	3099	10						12		10	
G-I	Edison											1207
	Fringe				96		21	2066	62	343		881
J	Astoria	1171	16	310		320	322			167		757
	Edison	605			86		18					322
	Helix	240	220		15		88					1698
	NRG		11	121			455			855		
	NYPA	489	412									
	Fringe	900					481					
K	LIPA	537	147	1376			532		120			2355
	NYPA	148	46	5								
	Fringe	53	95	15	17	29						

**Table 4:** Firms' Hydropower ( $Y_{i,n,w}$ ) Installed Capacities (MW).

$n$	$i$	PH	RR	RS
QC	HQ		13517	22583
A-E	NYPA	240	3957	
	Fringe		760	
F	NYPA	1160	23	
	Fringe		477	
G-I	NYPA		48	
	Fringe		59	

released from the upstream RS, thereby rendering a maximum annual production potential of 170 TWh, i.e., the historical average (Denault et al., 2009). On top of this, (14) regulates minimum annual water usage at each node for each hydro producer, e.g.,  $\bar{R}_{i,n}$  is 165 TWh for HQ based on the heritage pool (Hydro-Québec, 2019a).

Other data are wind production,  $R_{i,n,t}$ , and demand parameters,  $A_{n,t}$  and  $Z_{n,t}$ . There are 1,348 MW and 1,746 MW of wind capacity installed in Québec (CWEA, 2016) and at node A-E, respectively, with representative production profiles for the latter indicated in Figure 4a (NYISO, 2018). Estimated demand functions at an average price-quantity point<sup>11</sup> for each representative hour use an elasticity of demand of -0.065 (Debia et al., 2018) given hourly loads and prices (NYISO, 2018; NPCC, 2016; Régie de l'énergie Québec, 2019). Representative values for the inverse-demand intercept for zone J (New York City) are in Figure 4b.

In order to implement computationally tractable problem instances, we select a representative week per season (Reichenberg et al., 2018), i.e., four times 168 hours, that reflects the normalized seasonal-weekly values for wind output, demand, price, and exogenous imports.<sup>12</sup> We use the

<sup>11</sup>The Québec price is regulated to \$37.50/MWh. However, in order to explore the impact of potentially strategic use of storage, we use estimated demand functions for Québec in our Nash-Cournot framework.

<sup>12</sup>The use of representative weeks necessitates auxiliary intra-seasonal water-balance constraints analogous to (10) that account for net inflows during each season to apply to the reservoir-level variable of the previous season, scaled up by the duration of each season (typically the number of weeks in the season). For sake of exposition, we abstract from

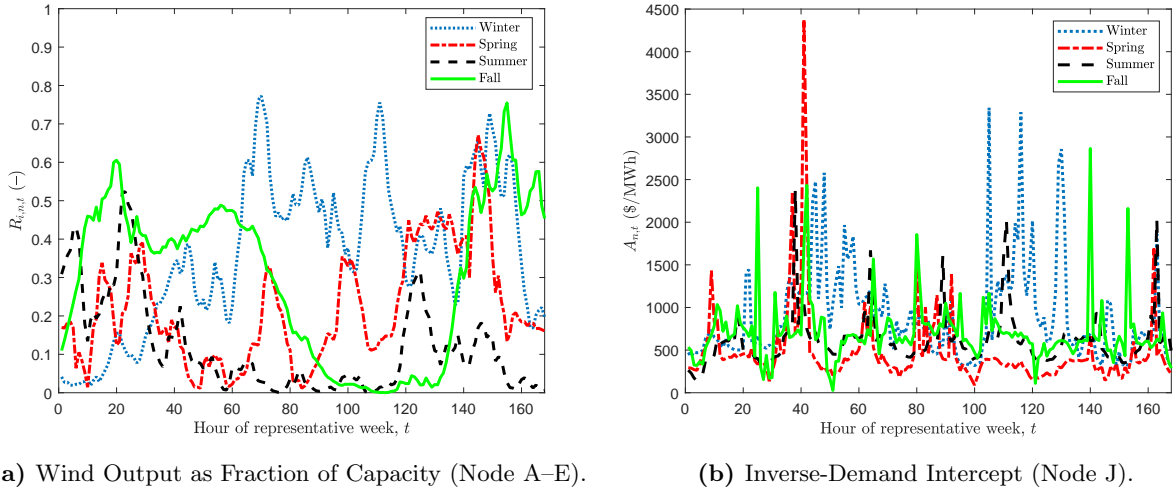


**Figure 4:** Clustered Representative-Week Seasonal Inputs.

Euclidean distance of the normalized values from the centroid of the dataset, which is composed of our criterion for representativity, i.e., the seasonal-weekly values of averages and standard errors. Thus, the representative week must be the closest to the expected value and volatility in a season, which is obtained by selecting the week minimizing the distance from each season’s centroid.

#### 4.2. Problem Instances

We implement problem instances for the following three market settings:

1. PC: all firms behave perfectly competitively.
2. CO-B2003: same as PC except that all firms apart from the fringe behave à la Cournot and Cournot hydro producers’ net-hydro production must meet a minimum level, reflecting the regulation of [Bushnell \(2003\)](#).<sup>13</sup>
3. CO-B2003-NI: same as CO-B2003 except that Cournot hydro producers’ net-hydro production plus net imports are regulated in (14).

These instances are selected to reflect (i) the notional benchmark, PC, (ii) the “literature” benchmark, CO-B2003, and (iii) our generalization of [Bushnell \(2003\)](#) to multiple nodes, CO-B2003-NI.

#### 4.3. Calibration

Figure 5 illustrates model calibration based on 2018 New York market prices. Here, the observed hourly prices in zone J (New York City) for the representative week for each season are displayed along with results of PC, CO-B2003, and CO-B2003-NI base-case problem instances.<sup>14</sup> According to

---

presenting the details.

<sup>13</sup>The net imports are deleted from (14).

<sup>14</sup>All problem instances take a few seconds to solve to optimality with GAMS 25.1.1 using CPLEX 12.8 deployed on an Intel Core i7-8650U CPU@1.90GHz quad-core processor and 16.0 GB of RAM.

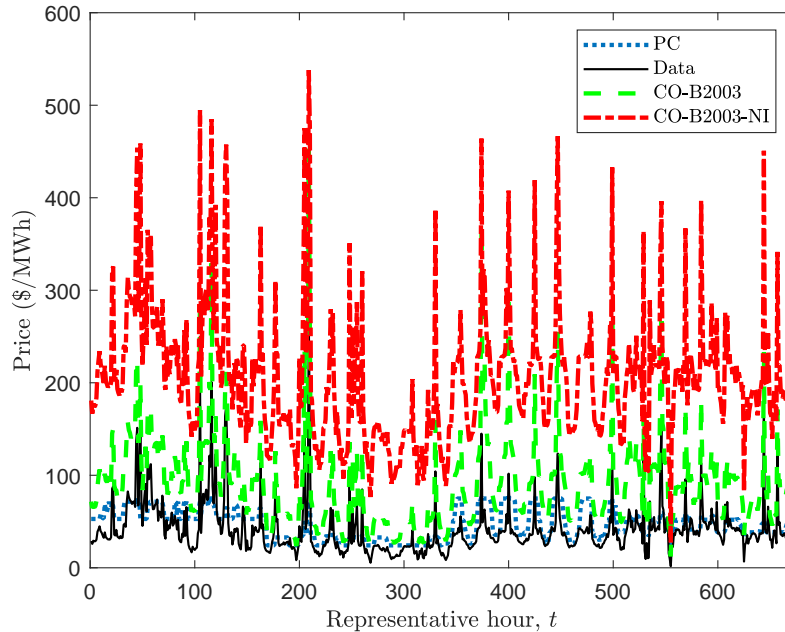


**Figure 5:** Price Calibration for New York City (Zone J).

our PC instance, the *average price* fits well with perfect competition in line with market analysis (Potomac Economics, 2019).<sup>15</sup> Yet, modeled prices in our other instances tend to be higher downstate, mostly because of Cournot behavior in zone J and the dominant position of LIPA in zone K. It is plausible that our Nash-Cournot model does not reflect the gamut of complex real-world rules that mitigate market power in the actual bidding process. However, since our objective is to study the impact of the strategic use of storage in a network, i.e., the spatio-temporal capability to shift energy, our modeled prices need to capture *price variation* more than the *price level*.

Toward this end, Table 5 displays the coefficient of determination for each instance and, thus, the explanatory power of our model.<sup>16</sup> The PC instance is actually inadequately reflective of price variation, especially for upstate New York where most of New York’s hydro capacity is concentrated. By contrast, the CO-B2003 instance is better at explaining downstate price variation, where the bulk of generation capacity is natural-gas based. In the context of our model, this indicates that price variation is determined by the marginal utility of the consumer rather than marginal cost, i.e., evidence of market power. Still, the ability to explain upstate price variation is not convincing. Using the CO-B2003-NI instance improves this latter metric substantially from 0.19 to 0.51. This suggests that when hydro regulation takes into account the spatial component, i.e., net imports at

<sup>15</sup>“Overall, the patterns of unoffered capacity and output gap were generally consistent with expectations in a competitive market and did not raise significant concerns regarding potential physical or economic withholding under most conditions.”

<sup>16</sup>The coefficient of determination measures the proportion of price variation explained by the model. The coefficient is computed via univariate OLS over price results against observed data. The instances with lowest cardinality account for 672. All coefficients are significantly different from zero with probability  $\gg 99.99\%$ .



**Table 5:** Coefficient of Determination for Modeled Prices.

Setting \ Zone	Zone								
	NYISO	A-I	J-K	A-E	F	G-I	J	K	
PC	0.32	0.16	0.45	0.16	0.16	0.15	0.44	0.45	
CO-B2003	0.55	0.19	0.89	0.20	0.18	0.18	0.91	0.88	
CO-B2003-NI	0.70	0.51	0.87	0.53	0.49	0.52	0.94	0.81	

each node, the marginal utility over the entire network becomes substantially more explicative of price variation. Consequently, it demonstrates that hydro producers tend to exert market power over the full network. Furthermore, the model’s overall explanatory power increases to 0.70, i.e., 70% of the price variation is explained by the CO-B2003-NI instance, which provides a credible basis for analyzing market power. Overall, our models confirm that the real market lies somewhere between perfect competition and Cournot oligopoly. Indeed, while price levels seem competitive, price variations are determined by marginal utility instead of marginal cost.

#### 4.4. Results

We present results for the three settings defined in Section 4.2 assuming both the existing CO<sub>2</sub> cap of 29.2 Mt (Section 4.4.1) and no CO<sub>2</sub> cap (Section 4.4.2). Corresponding results with a future CO<sub>2</sub> cap of 14.6 Mt, i.e., half of the current level or roughly an 80% reduction from 1990 levels, are provided in Appendix B.

##### 4.4.1. Base Case

Relative to the PC results in Table 6, Cournot behavior in CO-B2003 generally results in a loss in welfare with a net transfer from consumers to producers.<sup>17</sup> In particular, the temporal arbitrage by hydro producers detected in Bushnell (2003) is evidenced here via Figures 6 and 8 as HQ shifts production away from winter and summer, which are peak consumption seasons, in order to boost prices. Since HQ is unable to withhold water due to the regulation that it must produce at least 165 TWh annually, it endeavors to move the excess to a relatively off-peak season such as spring. Intuitively, HQ’s temporal arbitrage increases prices in the peak seasons by more than it depresses them in the off-peak one, thereby bolstering its profit. In fact, HQ even becomes a net importer of energy during the summer from zones A–E (Figure 9), which enables the strategic thermal firm there, NRG, to increase its profit via exports (especially in the summer) to create local scarcity (Debia et al., 2018). However, the CO<sub>2</sub> emission price,  $\rho$ , (which is the dual variable for the C&T constraint (13)) decreases under CO-B2003 vis-à-vis PC due to NRG’s withholding production overall in order to boost profit.

The imposition of water regulation that includes both net-hydro production and net imports under CO-B2003-NI improves Québec’s CS and SW by forcing HQ to increase its net-hydro production

<sup>17</sup>SW: social welfare, CS: consumer surplus, PS: producer surplus, MS: merchandising surplus, and GR: government revenue. We exclude the revenue from or cost of exogenous imports because the import revenue is not attributable to any agent in our region.

**Table 6:** Base-Case Results under Existing CO<sub>2</sub> Emission Cap (in Billion \$ Unless Indicated).

Setting \ Metric	PC	CO-B2003	CO-B2003-NI
SW	113.92	112.76	108.96
CS	104.89	99.49	93.02
PS	8.38	11.50	13.44
MS	0.44	1.75	-1.12
GR	0.21	0.02	3.63
$\rho$ (\$/t)	7.34	0.79	124.15
HQ Profit	5.03	6.38	5.07
NRG (A-E) Profit	0.04 (1.99)	0.22 (1.91)	0.59 (0.59)
LIPA Profit	0.08	0.33	1.22
NYPA Profit	0.85	1.13	1.28

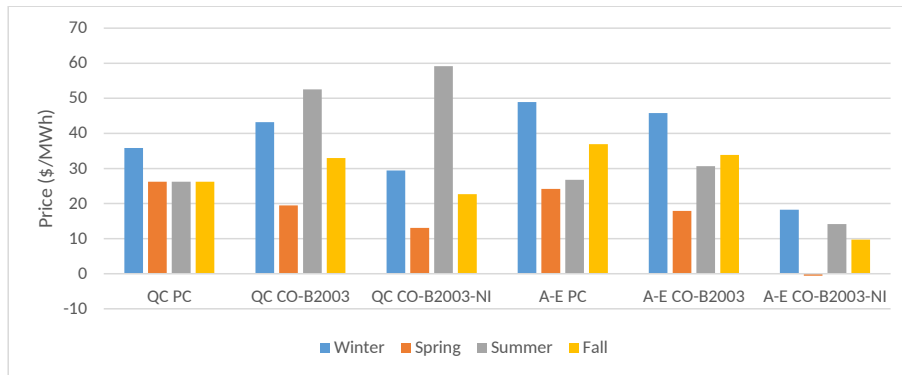


**Figure 6:** Impact of Market Power on Prices in Zones QC and A-E.

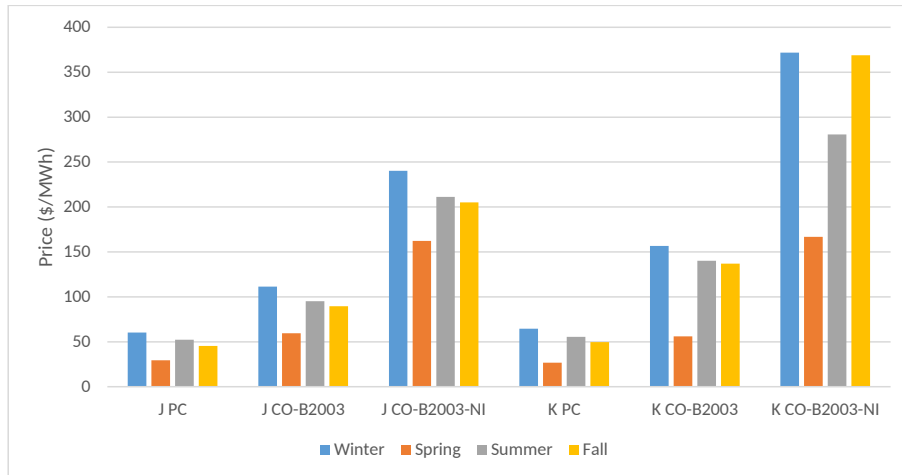


**Figure 7:** Impact of Market Power on Prices in Zones J and K.

and net imports in aggregate (Figure 10). However, it enables producers in downstate New York to increase prices (Figure 7) as they do not face competition from imports from Québec, which is also reflected in a higher CO<sub>2</sub> price. In effect, prices in zones A-E crash compared to those in

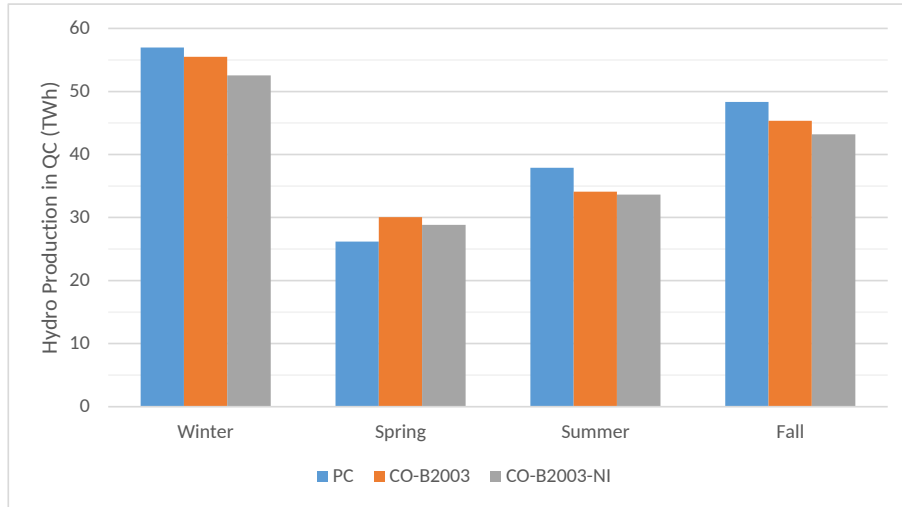


**Figure 8:** Impact of Market Power on Hydro Production in QC.

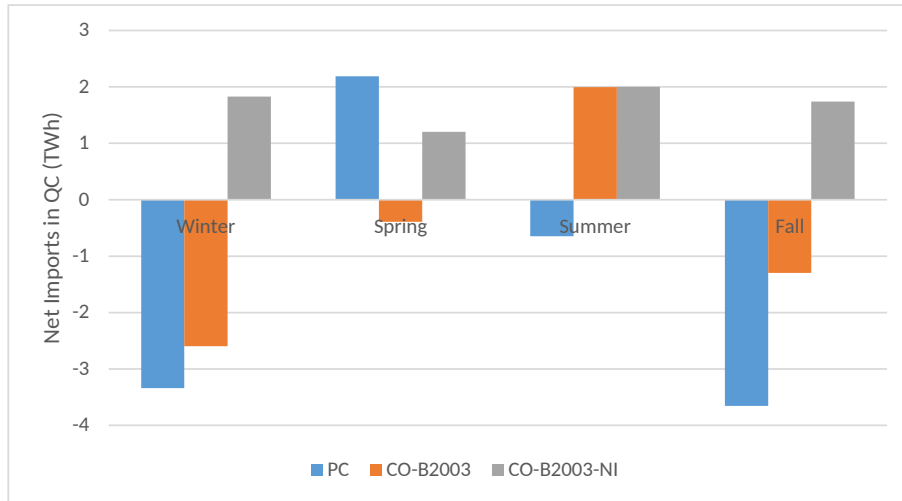


**Figure 9:** Impact of Market Power on Net Imports in QC.

zones J and K, which hints at the exercise of spatial arbitrage. Examining Tables 3 and 4, NYPA is a plausible beneficiary of a higher price differential between these upstate and downstate zones because it owns thermal capacity at the latter and PH capacity at the former. As indicated by Figure 11, NYPA increases PH operations in zones A–E, which provides a sink in which to “dump” energy produced elsewhere. Thus, higher net imports in zones A–E (Figure 12) and higher exports from zone J (Figure 13) decrease and increase local prices, respectively, thereby facilitating spatial arbitrage. Finally, reduced hydro exports from Québec cause the CO<sub>2</sub> emission price to increase drastically under CO-B2003-NI vis-à-vis PC and CO-B2003.

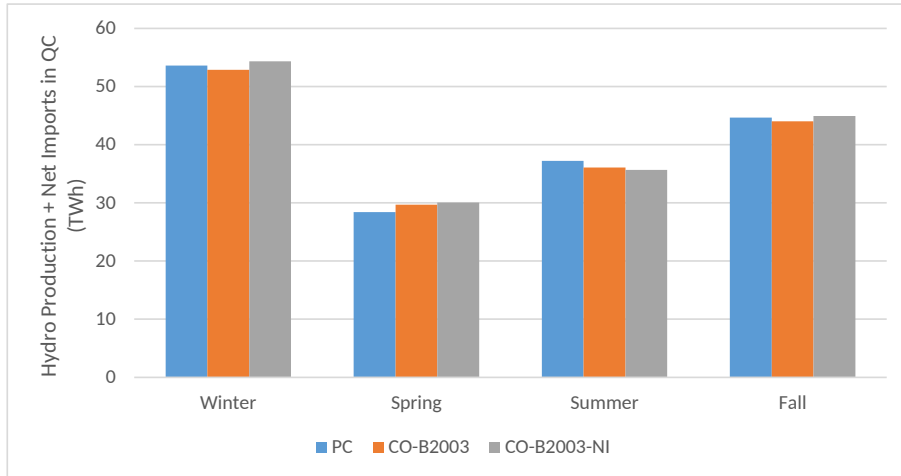


**Figure 10:** Impact of Market Power on Hydro Production and Net Imports in QC.

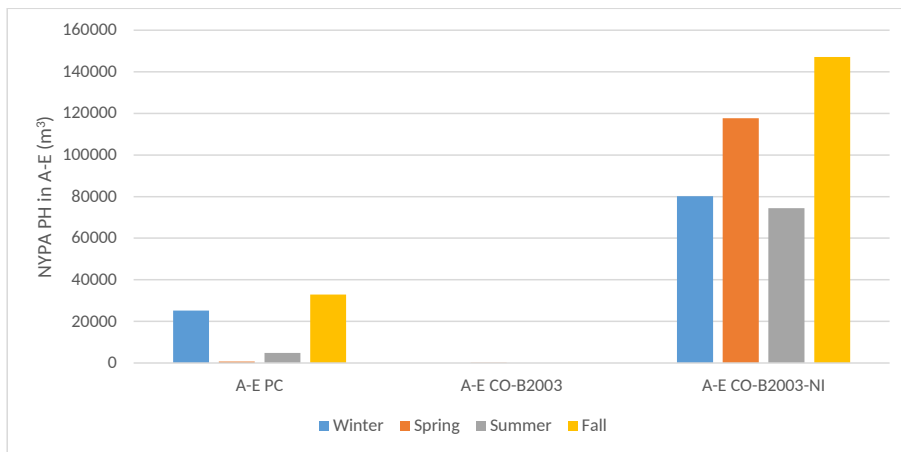


**Figure 11:** Impact of Market Power on Pumped Hydro Operations by NYPA in Zone A-E.

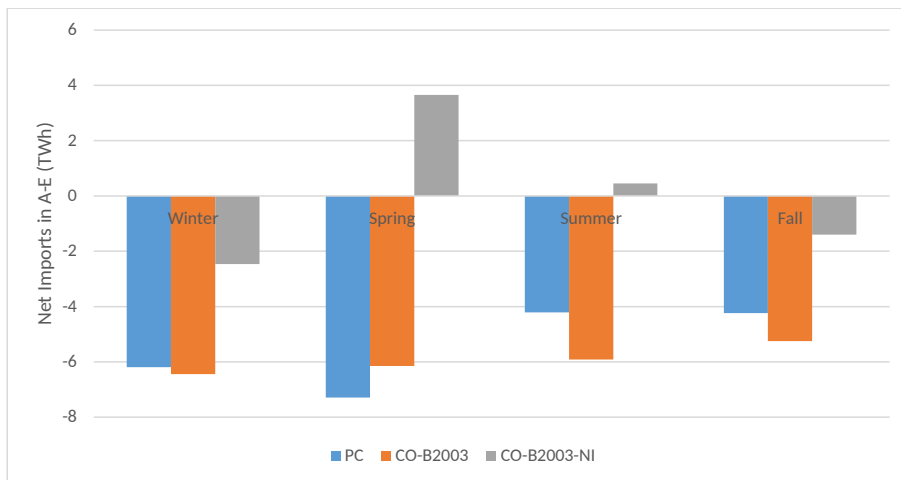


**Figure 12:** Impact of Market Power on Net Imports in Zone A-E.

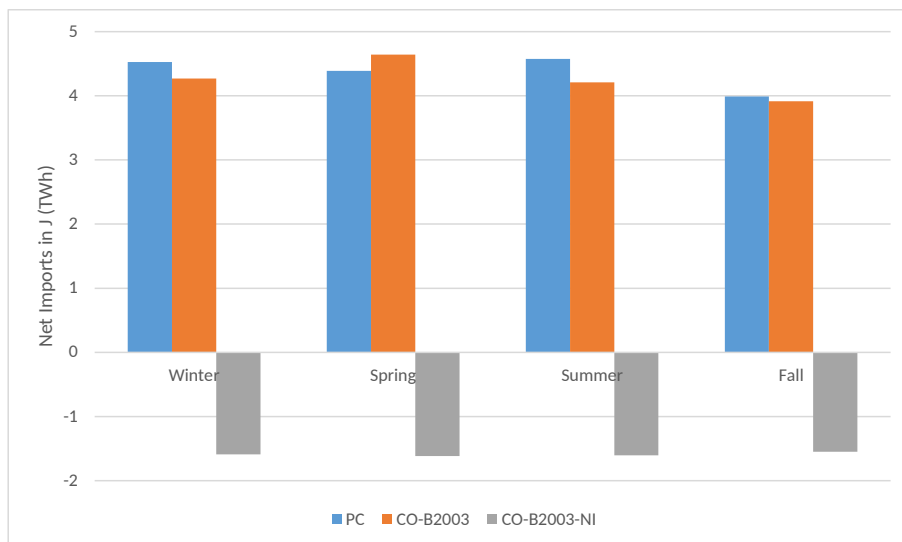


**Figure 13:** Impact of Market Power on Net Imports in Zone J.

**Table 7:** Results without CO<sub>2</sub> Emission Cap (in Billion \$ Unless Indicated).

Setting \ Metric	PC	CO-B2003	CO-B2003-NI
SW	114.03	112.78	110.09
CS	106.02	99.60	96.98
PS	7.58	11.42	13.88
MS	0.43	1.75	-0.77
EM (Mt)	32.01	30.35	36.28
HQ Profit	4.56	6.33	5.06
NRG (A–E) Profit	0.04 (1.77)	0.22 (1.88)	0.75 (0.52)
LIPA Profit	0.08	0.33	1.60
NYPA Profit	0.76	1.13	1.38

#### 4.4.2. No Carbon Cap

Since the role of the C&T was not covered by [Bushnell \(2003\)](#), we examine its impact on the firms’ incentives and the effectiveness of regulation by simply removing the cap on CO<sub>2</sub> emissions (Table 7, where “EM” refers to emissions). Under PC, removal of the cap boosts CS but lowers PS, especially that of HQ. It also tends to decrease exports from Québec (Figure 14) and reduces HQ’s hydro production in the summer, although it goes up in other seasons. Moving to CO-B2003 from PC still reveals a [Bushnell \(2003\)](#)-like effect (Figures 15–16), but the price increase in zones J and K under CO-B2003-NI (Figure 17) is less severe than under a carbon cap. Intuitively, this is due to the fact that fringe New York thermal producers can increase output more in response to the strategic producers’ efforts to raise prices without a carbon cap. Likewise, the imposition of the regulation on HQ’s net-hydro production plus net imports in CO-B2003-NI is more effective without the carbon cap as it even limits reduction in overall CS relative to its value under CO-B2003. Hence, attaining more ambitious climate targets in the presence of firms with market power with access to storage or transmission is likely to bolster their ability to exert spatial or temporal arbitrage and weaken the effectiveness of the regulation deployed under CO-B2003-NI.

## 5. Conclusions

Increased VRES penetration and stringent cuts to CO<sub>2</sub> emissions could provide more leverage to flexible thermal and hydro producers to exert market power. Such incentives may be enhanced particularly in power systems that are endowed with diversified power companies with a portfolio of flexible assets or hydro reservoirs as found empirically to be the case in the Iberian and Nordic regions ([Ito and Reguant, 2016](#); [Tangerås and Mauritzen, 2018](#)). It is plausible for similar distortions to arise from the ambitious sustainability targets posited by RGGI due to the interconnection with Québec’s large hydro reservoirs. While bottom-up equilibrium models have explored the impact of market power by flexible producers ([Debia et al., 2018](#); [Virasjoki et al., 2018](#)), they have tended to simplify the representation of the transmission network or hydro operations, thereby potentially not detecting strategies for spatial and temporal arbitrage.

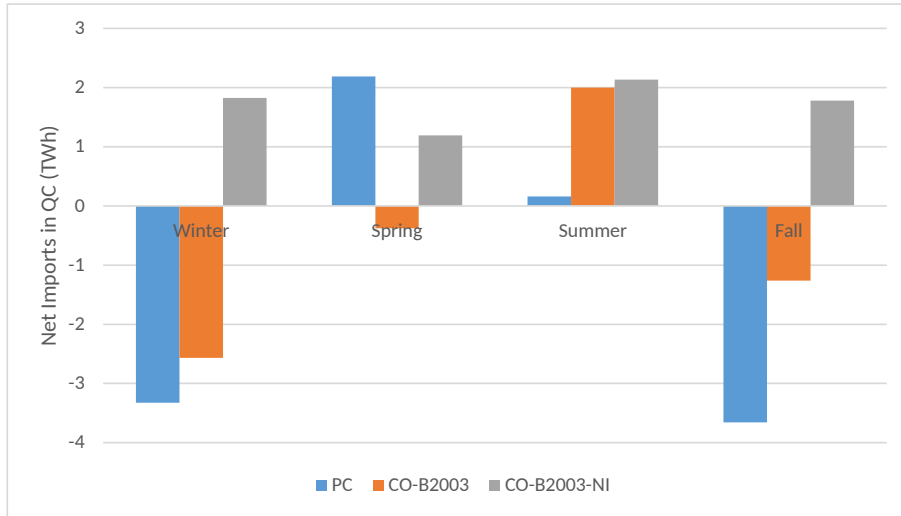


**Figure 14:** Impact of Market Power on Net Imports in QC without C&T.

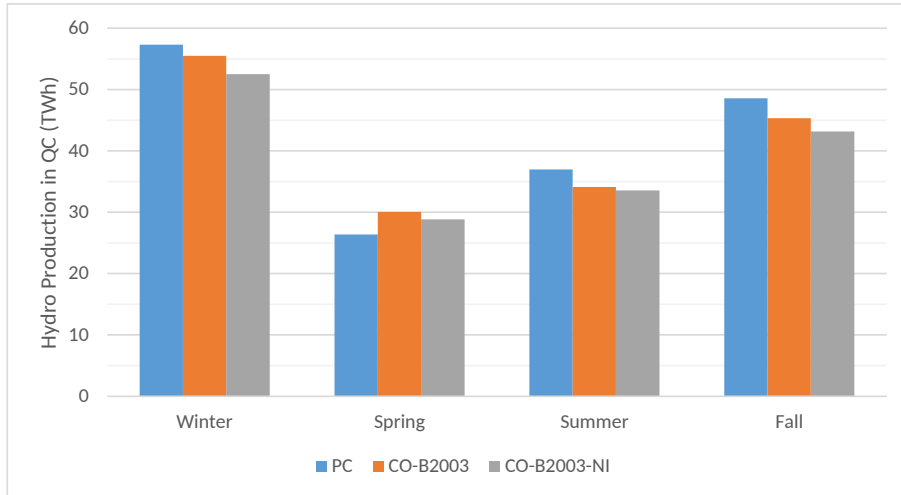


**Figure 15:** Impact of Market Power on Hydro Production in QC without C&T.

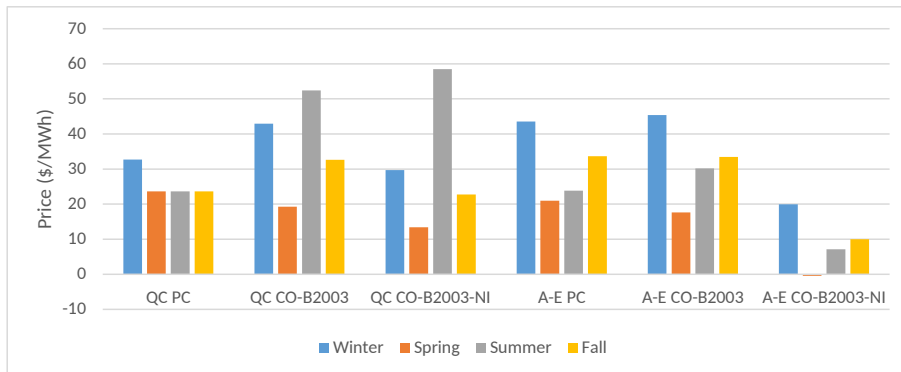


**Figure 16:** Impact of Market Power on Prices in Zones QC and A-E without C&T.

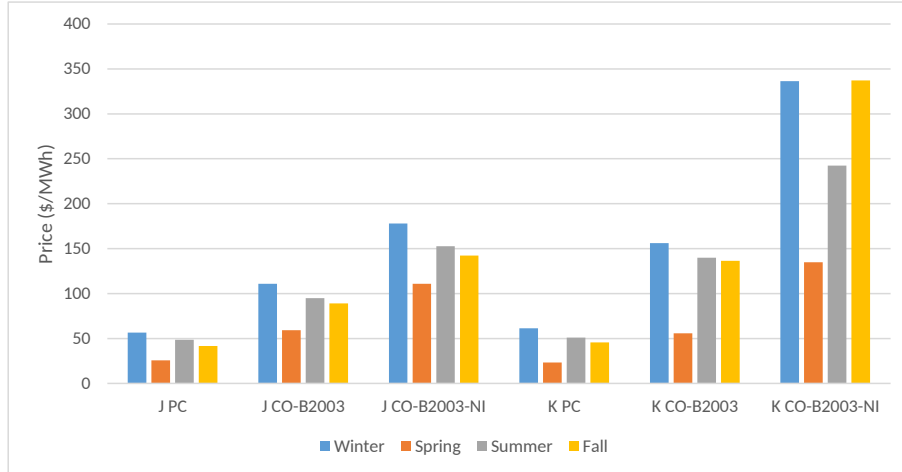


**Figure 17:** Impact of Market Power on Prices in Zones J and K without C&T.

Using a credibly calibrated equilibrium model of the New York and Québec power systems with an adequate representation of producer behavior, power flows, hydro reservoirs, and seasonal variation in demand and VRES, we have demonstrated how production flexibility may be exploited. In particular, we have obtained the following economic insights alluded to in Section 1 that could inform future energy policy in the region:

- (i) Under a minimum water-usage constraint à la [Bushnell \(2003\)](#), a large hydro producer may be able to exercise *temporal arbitrage* by moving water from peak to off-peak seasons. In tandem, thermal producers in New York may strategically withhold output in order to raise the electricity price, which would cause the CO<sub>2</sub> emission price to decrease significantly.
- (ii) Water regulation comprising net imports mitigates this *temporal arbitrage* but could actually open the possibility for *spatial arbitrage* by a firm that owns both thermal and PH facilities. In effect, such a firm would export power from the node with thermal generation to the node with PH, i.e., raising the price at the former by creating scarcity and exploiting the lower price at the latter to “destroy” energy via PH. Combined with HQ’s reduced exports to New York, such a water-usage regulation could actually cause the CO<sub>2</sub> emission price to increase.
- (iii) More ambitious environmental targets are likely to reduce the effectiveness of such water regulation as price-taking thermal generation is less able to respond to price signals due to the C&T restriction.

Our bottom-up equilibrium framework is an open-loop Cournot model for analyzing operational decisions over a medium-term horizon, i.e., a given test year. As such, it makes simplifying assumptions about uncertainty and plant operations even if it is able to explain seasonal variations in nodal prices well. Directions for future work include either improving the representation of seasonal variability ([Tejada-Arango et al., 2018](#)) or formalizing the insights in a more realistic but computationally intensive closed-loop setting incorporating uncertainty ([Conejo et al., 2016](#)).



Looking beyond fixed capacities, allowing for investment decisions, e.g., in generation, storage, and transmission capacities, would be especially pertinent given future climate targets. All of these avenues would require a bi-level modeling approach as would an analysis of optimal environmental or water regulation (Siddiqui et al., 2016).

## Appendix A KKT Conditions

From (1)-(5) after internalization of  $\gamma_{i,n}$  from equilibrium constraint (14), the ISO's KKT conditions are:

$$0 \leq c_{n,t} \perp \lambda_{n,t} - A_{n,t} + Z_{n,t} c_{n,t} \geq 0, \forall n, t \quad (\text{A-1})$$

$$f_{\ell,t} \text{ free}, \psi_{\ell,t} + V \left( \lambda_{n_{\ell}^+,t} - \lambda_{n_{\ell}^-,t} - \underline{\mu}_{\ell,t} + \bar{\mu}_{\ell,t} + \sum_{i \in \mathcal{I}_{n_{\ell}^+,w}} \gamma_{i,n_{\ell}^+} - \sum_{i \in \mathcal{I}_{n_{\ell}^-,w}} \gamma_{i,n_{\ell}^-} \right) = 0, \forall \ell, t \quad (\text{A-2})$$

$$v_{n,t} \text{ free}, - \sum_{\ell \in \mathcal{L}_n^+} B_{\ell} \psi_{\ell,t} + \sum_{\ell \in \mathcal{L}_n^-} B_{\ell} \psi_{\ell,t} - \underline{\kappa}_{n,t} + \bar{\kappa}_{n,t} = 0, \forall n, t \quad (\text{A-3})$$

$$\lambda_{n,t} \text{ free}, c_{n,t} - \sum_{i \in \mathcal{I}} q_{i,n,t} - V \left( \sum_{\ell \in \mathcal{L}_n^-} f_{\ell,t} - \sum_{\ell \in \mathcal{L}_n^+} f_{\ell,t} \right) = 0, \forall n, t \quad (\text{A-4})$$

$$\psi_{\ell,t} \text{ free}, f_{\ell,t} - B_{\ell} \left( v_{n_{\ell}^+,t} - v_{n_{\ell}^-,t} \right) = 0, \forall t, \ell \in \mathcal{L}^{AC} \quad (\text{A-5})$$

$$0 \leq \underline{\mu}_{\ell,t} \perp K_{\ell} + V f_{\ell,t} \geq 0, \forall t, \ell \quad (\text{A-6})$$

$$0 \leq \bar{\mu}_{\ell,t} \perp K_{\ell} - V f_{\ell,t} \geq 0, \forall t, \ell \quad (\text{A-7})$$

$$0 \leq \underline{\kappa}_{n,t} \perp \pi + v_{n,t} \geq 0, \forall t, n \quad (\text{A-8})$$

$$0 \leq \bar{\kappa}_{n,t} \perp \pi - v_{n,t} \geq 0, \forall t, n \quad (\text{A-9})$$

From (6)-(12) after internalization of  $\rho$  and  $\gamma_{i,n}$  from equilibrium constraints (13) and (14), respectively, firm  $i$ 's KKT conditions are:

$$q_{i,n,t} \text{ free}, \xi_{i,n,t} - A_{n,t} + Z_{n,t} \left[ \sum_{i' \in \mathcal{I}} q_{i',n,t} + V \left( \sum_{\ell \in \mathcal{L}_n^-} f_{\ell,t} - \sum_{\ell \in \mathcal{L}_n^+} f_{\ell,t} \right) \right] + Z_{n,t} q_{i,n,t} = 0, \forall n, t \quad (\text{A-10})$$

$$0 \leq g_{i,n,t,u} \perp -\xi_{i,n,t} + (C_{i,n,t,u} + \rho E_{i,n,u}) + \beta_{i,n,t,u} + \left( \bar{\beta}_{i,n,t,u} - \underline{\beta}_{i,n,t,u} \right) + \left( \underline{\beta}_{i,n,t+1,u} - \bar{\beta}_{i,n,t+1,u} \right) \geq 0, \forall n, t, u \in \mathcal{U}_{i,n} \quad (\text{A-11})$$

$$0 \leq s_{i,n,t,w} \perp F_{i,n,w} (\xi_{i,n,t} + \gamma_{i,n}) - \alpha_{i,n,t+1,w} + \sum_{w' \in \mathcal{C}(w)} \alpha_{i,n,t,w'} \geq 0, \forall n, t, w \in \mathcal{W}_{i,n} \quad (\text{A-12})$$

$$0 \leq y_{i,n,t,w} \perp P_{i,n,w} (\delta_{i,n,t,w} - \xi_{i,n,t} - \gamma_{i,n}) + \alpha_{i,n,t,w} - \sum_{w' \in \mathcal{C}(w)} \alpha_{i,n,t+1,w'} \geq 0, \forall n, t, w \in \mathcal{W}_{i,n} \quad (\text{A-13})$$

$$0 \leq z_{i,n,t,w} \perp \alpha_{i,n,t,w} - \sum_{w' \in \mathcal{C}(w)} \alpha_{i,n,t+1,w'} \geq 0, \forall n, t, w \in \mathcal{W}_{i,n} \quad (\text{A-14})$$

$$0 \leq x_{i,n,t,w} \perp -\alpha_{i,n,t+1,w} + \alpha_{i,n,t,w} - \underline{\omega}_{i,n,t,w} + \bar{\omega}_{i,n,t,w} \geq 0, \forall n, t, w \in \mathcal{W}_{i,n} \quad (\text{A-15})$$

$$\xi_{i,n,t} \text{ free, } q_{i,n,t} - \left[ \sum_{u \in \mathcal{U}_{i,n}} g_{i,n,t,u} + R_{i,n,t} + \sum_{w \in \mathcal{W}_{i,n}} (P_{i,n,w} y_{i,n,t,w} - F_{i,n,w} s_{i,n,t,w}) \right] = 0, \forall n, t \quad (\text{A-16})$$

$$0 \leq \beta_{i,n,t,u} \perp G_{i,n,t,u} - g_{i,n,t,u} \geq 0, \forall n, t, u \in \mathcal{U}_{i,n} \quad (\text{A-17})$$

$$0 \leq \underline{\beta}_{i,n,t,u} \perp -\underline{G}_{i,n,t,u} + g_{i,n,t,u} - g_{i,n,t-1,u} \geq 0, \forall n, t, u \in \mathcal{U}_{i,n} \quad (\text{A-18})$$

$$0 \leq \bar{\beta}_{i,n,t,u} \perp \bar{G}_{i,n,t,u} - g_{i,n,t,u} + g_{i,n,t-1,u} \geq 0, \forall n, t, u \in \mathcal{U}_{i,n} \quad (\text{A-19})$$

$$\alpha_{i,n,t,w} \text{ free, } x_{i,n,t,w} - I_{i,n,t,w} - x_{i,n,t-1,w} + (y_{i,n,t,w} + z_{i,n,t,w} - s_{i,n,t-1,w}) - \sum_{w' \in \mathcal{A}(w)} (y_{i,n,t-1,w'} + z_{i,n,t-1,w'} - s_{i,n,t,w'}) = 0, \forall n, t, w \in \mathcal{W}_{i,n} \quad (\text{A-20})$$

$$0 \leq \underline{\omega}_{i,n,t,w} \perp -\underline{X}_{i,n,w} + x_{i,n,t,w} \geq 0, \forall n, t, w \in \mathcal{W}_{i,n} \quad (\text{A-21})$$

$$0 \leq \bar{\omega}_{i,n,t,w} \perp \bar{X}_{i,n,w} - x_{i,n,t,w} \geq 0, \forall n, t, w \in \mathcal{W}_{i,n} \quad (\text{A-22})$$

$$0 \leq \delta_{i,n,t,w} \perp Y_{i,n,w} - P_{i,n,w} y_{i,n,t,w} \geq 0, \forall n, t, w \in \mathcal{W}_{i,n} \quad (\text{A-23})$$

The equilibrium constraints in (13)–(14) are rendered as complementarity conditions to complete the MCP:

$$0 \leq \rho \perp \bar{E} - \sum_{i \in \mathcal{I}} \sum_{n \in \mathcal{N}} \sum_{t \in \mathcal{T}} \sum_{u \in \mathcal{U}_{i,n}} E_{i,n,u} g_{i,n,t,u} \geq 0 \quad (\text{A-24})$$

$$0 \leq \gamma_{i,n} \perp \sum_{t \in \mathcal{T}} \left[ \sum_{w \in \mathcal{W}_{i,n}} (P_{i,n,w} y_{i,n,t,w} - F_{i,n,w} s_{i,n,t,w}) + V \left( \sum_{\ell \in \mathcal{L}_n^-} f_{\ell,t} - \sum_{\ell \in \mathcal{L}_n^+} f_{\ell,t} \right) \right] - \bar{R}_{i,n} \geq 0, \forall i, n \in \mathcal{N}_{i,w} \quad (\text{A-25})$$

## Appendix B Low Carbon Cap

We run a case with a cap of 14.6 Mt on CO<sub>2</sub> emissions, which is half that in the base case. This is roughly in line with the 80% reduction from 1990 levels envisaged in most future climate targets. However, since such a drastic transformation of the power sector would necessitate investments in new generation and transmission capacity, results for such a future scenario should be treated with caution. Indeed, ours is a medium-term equilibrium model that focuses only on the operational aspects, which is why the following results should be taken with the appropriate caveats. As expected, the tighter carbon cap decreases SW and CS in all settings (Table B-1) as the cost of emissions is internalized in the form of higher prices (Figures B-1–B-2). Since the existing generation and transmission configuration must meet the ambitious CO<sub>2</sub> target, the CO<sub>2</sub> emission price soars, which benefits PS under the PC and CO-B2003 settings. Such an exorbitant price on CO<sub>2</sub> emissions also curbs consumption, which harms PS under CO-B2003-NI. Compared to the base case, HQ is obligated to increase its production and exports (Figures B-3–B-4). A thorough analysis of future

**Table B-1:** Results with a Low CO<sub>2</sub> Emission Cap (in Billion \$ Unless Indicated).

Setting \ Metric	PC	CO-B2003	CO-B2003-NI
SW	111.55	110.57	103.29
CS	91.25	87.34	85.78
PS	16.15	18.60	10.47
MS	1.55	2.29	-1.32
GR	2.61	2.34	8.35
$\rho$ (\$/t)	178.49	160.56	572.25
HQ Profit	8.72	10.39	5.13
NRG (A-E) Profit	0.02 (4.88)	0.10 (4.88)	0.08 (0.55)
LIPA Profit	0.10	0.25	0.41
NYPA Profit	1.97	2.06	0.73

climate targets would necessitate inclusion of investment decisions. For example, [Rodríguez-Sarasty et al. \(2021\)](#) analyze investment in new generation and transmission in New York, Québec, and the entire North-East region under tighter carbon constraints. Such results are, however, obtained under perfect competition.

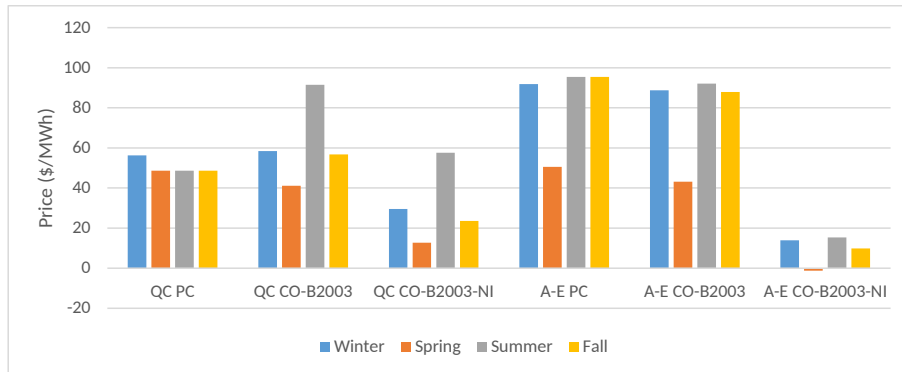


**Figure B-1:** Impact of Market Power on Prices in Zones QC and A-E under a Low Carbon Cap.

## Acknowledgements

This work has been supported by funding received from the Social Sciences and Humanities Research Council (SSHRC) of Canada under grant number 435-2017-0068 and HEC Montréal’s Chair in Energy Sector Management. We have benefited from feedback received at the 2019 Workshop on Electricity Systems of the Future: Incentives, Regulation, and Analysis for Efficient Investment at the Isaac Newton Institute for the Mathematical Sciences (in particular from Andy Philpott and Ramteen Sioshansi), the 2019 International Conference of the International Association for Energy Economics, the 2019 Annual Meeting of the Institute for Operations Research and the Management Sciences, and a seminar at Concordia University. Comments from the handling editor and two anonymous referees have greatly improved the paper. All remaining errors are the authors’ own.

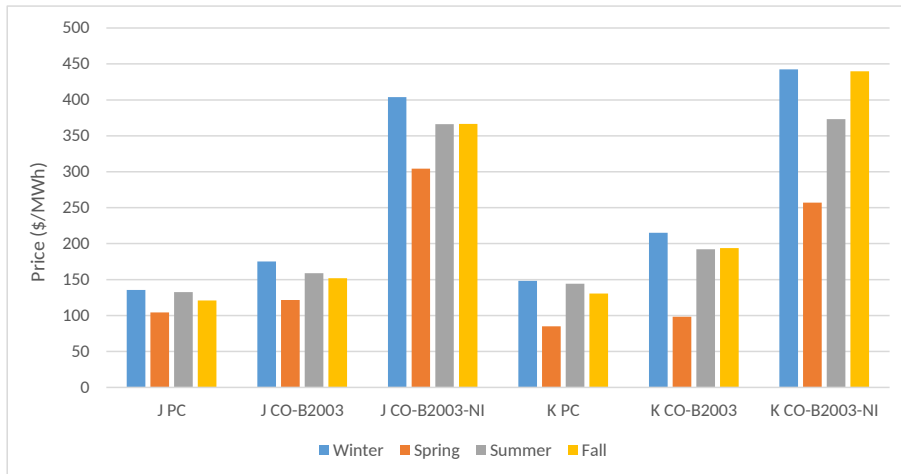


Figure B-2: Impact of Market Power on Prices in Zones J and K under a Low Carbon Cap.

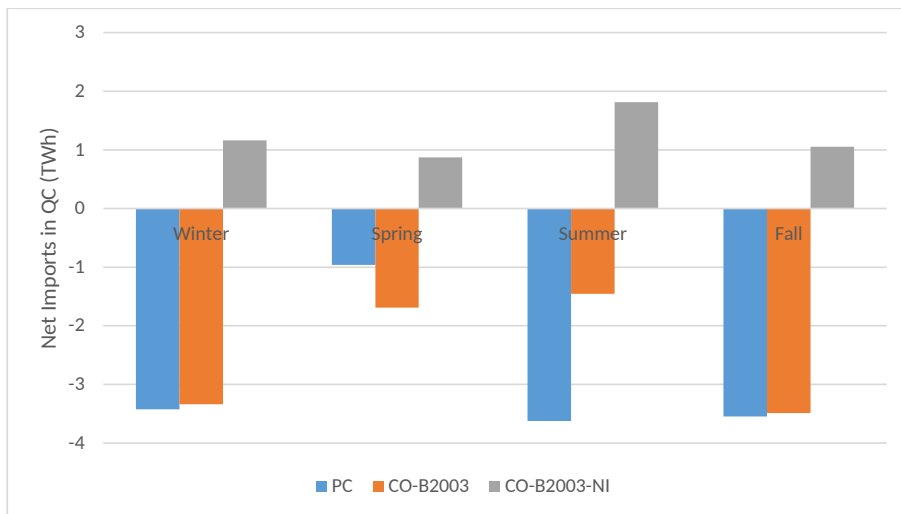


Figure B-3: Impact of Market Power on Net Imports in QC under a Low Carbon Cap.

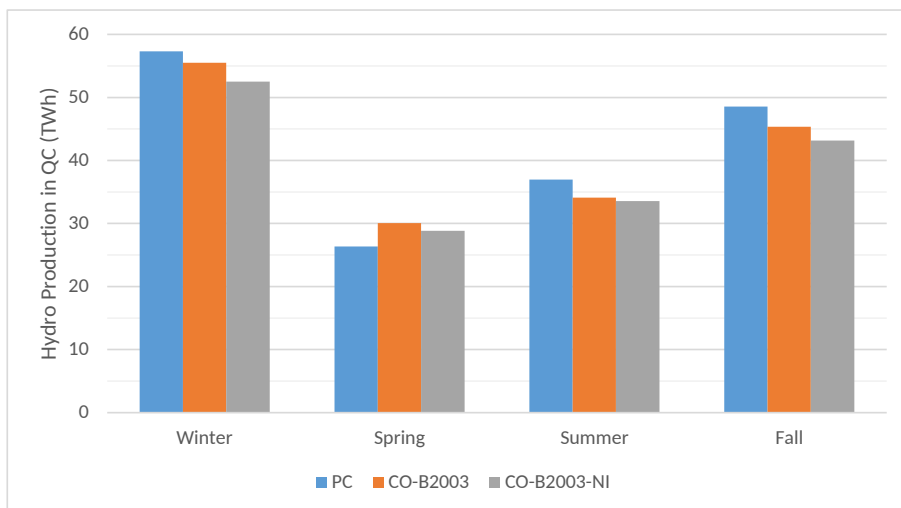


Figure B-4: Impact of Market Power on Hydro Production in QC under a Low Carbon Cap.

## References

- Aasgård, E.K., G.S. Andersen, S.-E. Fleten, and D. Haugstvedt (2014), “Evaluating a Stochastic-Programming-Based Bidding Model for a Multireservoir System,” *IEEE Trans. Power Syst.*, 29(4): 1748–1757.
- Bjørndal, E., M. Bjørndal, and H. Cai (2014), “Nodal Pricing in a Coupled Electricity Market,” *11th Intl. Conf. Eur. Ener. Mkts.*, pp. 1–6.
- Bouffard, F., S. Debia, N. Dhaliwal, and P.-O. Pineau (2018), *A Decarbonized Northeast Electricity Sector: The Value of Regional Integration*, [http://energie.hec.ca/wp-content/uploads/2018/06/ScopingStudy\\_NortheastHydroModelling\\_13june2018.pdf](http://energie.hec.ca/wp-content/uploads/2018/06/ScopingStudy_NortheastHydroModelling_13june2018.pdf).
- Bushnell, J. (2003), “A Mixed Complementarity Model of Hydrothermal Electricity Competition in the Western United States,” *Oper. Res.*, 51(1): 80–93.
- Bushnell, J. and Y. Chen (2012), “Allocation and Leakage in Regional Cap-and-Trade Markets for CO<sub>2</sub>,” *Res. & Ener. Econ.*, 34: 647–668.
- Conejo, A.J., L. Baringo, S.J. Kazempour, and A.S. Siddiqui (2016), *Investment in Electricity Generation and Transmission*, Springer International.
- Crampes, C. and M. Moreaux (2001), “Water Resource and Power Generation,” *Int. J. Ind. Org.*, 19(6): 975–997.
- CWEA (2016), *Pan-Canadian Wind Integration Study*, <https://canwea.ca/wind-integration-study/full-report/>.
- Debia, S., D. Benatia, and P.-O. Pineau (2018), “Evaluating an Interconnection Project: Do Strategic Interactions Matter?,” *The Energy J.*, 39(6): 73–94.
- Debia, S., P.-O. Pineau, and A.S. Siddiqui (2019), “Strategic Use of Storage: The Impact of Carbon Policy, Resource Availability, and Technology Efficiency on a Renewable-Thermal Power System,” *Ener. Econ.*, 80: 100–122.
- Denault, M., D. Dupuis, and S. Couture-Cardinal (2009), “Complementarity of Hydro and Wind Power: Improving the Risk Profile of Energy Inflows,” *Ener. Pol.*, 37(12): 5376–5384.
- Egerer, J. (2016), *Open Source Electricity Model for Germany (ELMOD-DE)*, [https://www.diw.de/documents/publikationen/73/diw\\_01.c.528927.de/diw\\_datadoc\\_2016-083.pdf](https://www.diw.de/documents/publikationen/73/diw_01.c.528927.de/diw_datadoc_2016-083.pdf).
- Energy Information Administration (2018), *Electric Power Annual 2017*, <https://www.eia.gov/electricity/annual/pdf/epa.pdf>.
- Finardi, E.C. and E.L. da Silva (2006), “Solving the Hydro Unit Commitment Problem via Dual Decomposition and Sequential Quadratic Programming,” *IEEE Trans. Power Syst.*, 21(2): 835–844.

- Flach, B.C., L.A. Barroso, and M.V.F. Pereira (2010), “Long-Term Optimal Allocation of Hydro Generation for a Price-Maker Company in a Competitive Market: Latest Developments and a Stochastic Dual Dynamic Programming Approach,” *IET Gen., Trans. & Dist.*, 4(2): 299–314.
- Førsund, F. (2015), *Hydropower Economics*, Springer.
- Gabriel, S. and F. Leuthold (2010), “Solving Discretely-Constrained MPEC Problems with Applications in Electric Power Markets,” *Ener. Econ.*, 32: 3–14.
- Gabriel, S.A., A.J. Conejo, J.D. Fuller, B.F. Hobbs, and C. Ruiz (2013), *Complementarity Modeling in Energy Markets*, Springer.
- Gonzalez-Salazar, M.A., T. Kirsten, and L. Prchlik (2018), “Review of the Operational Flexibility and Emissions of Gas- and Coal-Fired Power Plants in a Future with Growing Renewables,” *Ren. & Sust. Ener. Rev.*, 82: 1497–1513.
- Hashimoto, H. (1985), “A Spatial Nash Equilibrium Model,” in Harker, P.T., editor, *Spatial Price Equilibrium: Advances in Theory, Computation and Application*, pp. 20–40, Springer.
- Hirth, L. (2016), “The Benefits of Flexibility: The Value of Wind Energy with Hydropower,” *Appl. Ener.*, 181: 210–223.
- Hobbs, B.F. (2001), “Linear Complementarity Models of Nash-Cournot Competition in Bilateral and POOLCO Power Markets,” *IEEE Trans. Power Syst.*, 16(2): 194–202.
- Hydro-Québec (2019a), *Hydro-Québec Division Profile*, <http://www.hydroquebec.com/generation/profil.html>.
- Hydro-Québec (2019b), *Hydro-Québec Production*, <http://www.hydroquebec.com/production/>.
- IEA (2019), *Market Report Series: Renewables 2019 - Analysis and Forecasts to 2024*, <https://webstore.iea.org/market-report-series-renewables-2019>.
- Ito, K. and M. Reguant (2016), “Sequential Markets, Market Power, and Arbitrage,” *Amer. Econ. Rev.*, 106(7): 1921–1957.
- Lund, P.D., J. Lindgren, J. Mikkola, and J. Salpakari (2015), “Review of Energy System Flexibility Measures to Enable High Levels of Variable Renewable Electricity,” *Ren. & Sust. Ener. Rev.*, 45: 785–807.
- Moiseeva, E. and M.R. Hesamzadeh (2018), “Strategic Bidding of a Hydropower Producer Under Uncertainty: Modified Benders Approach,” *IEEE Trans. Power Syst.*, 33(1): 861–873.
- Monderer, D. and L.S. Shapley (1996), “Potential Games,” *Games & Econ. Behavior*, 14(1): 124–143.
- Murphy, F. and Y. Smeers (2005), “Generation Capacity Expansion in Imperfectly Competitive Restructured Electricity Markets,” *Oper. Res.*, 53(4): 646–661.

- Nasrolahpour, E., S.J. Kazempour, H. Zareipour, and W.D. Rosehart (2016), “Strategic Sizing of Energy Storage Facilities in Electricity Markets,” *IEEE Trans. Sust. Ener.*, 7: 1462–1472.
- NPCC (2016), *2016 Long Range Adequacy Overview*, [https://www.npcc.org/Library/Resource%20Adequacy/2016LongRangeOverview\(Approved%20by%20the%20RCC%20December%206%202016\).pdf](https://www.npcc.org/Library/Resource%20Adequacy/2016LongRangeOverview(Approved%20by%20the%20RCC%20December%206%202016).pdf).
- NYISO (2015), *2015 Load and Capacity Data*, <https://www.nyiso.com/documents/20142/2226467/2015-Load-Capacity-Data-Report-Gold-Book.pdf/63d6d932-7a50-4972-1cc9-e3f1eaa7ab90>.
- NYISO (2018), *2018 Power Trends*, <https://www.nyiso.com/documents/20142/2223020/2018-Power-Trends.pdf/4cd3a2a6-838a-bb54-f631-8982a7bdfa7a>.
- NYISO (2019), *Real-Time Fuel Mix*, <http://mis.nyiso.com/public/P-63list.htm>.
- New York State (2019), *New York State Climate Leadership and Community Protection Act*, <https://www.nysenate.gov/legislation/bills/2019/s6599>.
- NYSRC (2012), *New York Control Area Installed Capacity Requirements for the Period May 2011 through April 2012*, [http://www.nysrc.org/pdf/Reports/2011%20IRM%20Final%20Report%2012-10-10\[1\].pdf](http://www.nysrc.org/pdf/Reports/2011%20IRM%20Final%20Report%2012-10-10[1].pdf).
- Oggioni, G., Y. Smeers, E. Allevi, and S. Schaible (2012), “A Generalized Nash Equilibrium Model of Market Coupling in the European Power System,” *Net. & Spat. Econ.*, 12(4): 503–560.
- Potomac Economics (2019), *2018 State of the Market Report for the New York ISO Markets*, [https://www.potomaceconomics.com/wp-content/uploads/2019/05/NYISO-2018-SOM-Report\\_Full-Report\\_\\_5-8-2019\\_Final.pdf](https://www.potomaceconomics.com/wp-content/uploads/2019/05/NYISO-2018-SOM-Report_Full-Report__5-8-2019_Final.pdf).
- Ramos, A., M. Ventosa, and M. Rivier (1998), “Modeling Competition in Electric Energy Markets by Equilibrium Constraints,” *Util. Pol.*, 7: 233–242.
- Régie de l’énergie Québec (2019), *Entente globale cadre 2017–2019*, [http://www.regie-energie.qc.ca/audiences/Suivis/Suivi\\_HQD\\_D-2016-143.html](http://www.regie-energie.qc.ca/audiences/Suivis/Suivi_HQD_D-2016-143.html).
- Reichenberg, L., A.S. Siddiqui, and S. Wogrin (2018), “Policy Implications of Downscaling the Time Dimension in Power System Planning Models to Represent Variability in Renewable Output,” *Energy*, 159: 870–877.
- RGGI (2019), *The Regional Greenhouse Gas Initiative*, <https://www.rggi.org/>.
- Rodríguez-Sarasty, J.A., S. Debia, and P.-O. Pineau (2021), “Deep Decarbonization in Northeastern North America: the Value of Electricity Market Integration and Hydropower,” *Ener. Pol.*, 152: 112210.

- Rosen, J.B. (1965), “Existence and Uniqueness of Equilibrium Points for Concave N-Person Games,” *Econometrica*, 33(3): 520–534.
- Schill, W.-P. and C. Kemfert (2011), “Modeling Strategic Electricity Storage: The Case of Pumped Hydro Storage in Germany,” *The Energy J.*, 32: 59–88.
- Siddiqui, A.S., M. Tanaka, and Y. Chen (2016), “Are Targets for Renewable Portfolio Standards Too Low? The Impact of Market Structure on Energy Policy,” *Eur. J. Oper. Res.*, 250(1): 328–341.
- Siddiqui, A.S., R. Sioshansi, and A.J. Conejo (2019), “Merchant Storage Investment in a Restructured Electricity Industry,” *The Energy J.*, 40(4): 129–155.
- Singh, R. and A. Wiszniewska-Matyskiel (2019), “Discontinuous Nash Equilibria in a Two-Stage Linear-Quadratic Dynamic Game With Linear Constraints,” *IEEE Trans. Aut. Cont.*, 64(7): 3074–3079.
- Sioshansi, R. (2010), “Welfare Impacts of Electricity Storage and the Implications of Ownership Structure,” *The Energy J.*, 31(2): 173–198.
- Sioshansi, R. (2014), “When Energy Storage Reduces Social Welfare,” *Ener. Econ.*, 41: 106–116.
- Steinberg, D., D. Bielen, J. Eichman, K. Eurek, J. Logan, T. Mai, C. McMillan, A. Parker, L. Vimmerstedt, and E. Wilson (2017), *Electrification & Decarbonization: Exploring U.S. Energy Use and Greenhouse Gas Emissions in Scenarios with Widespread Electrification and Power Sector Decarbonization*, <https://www.nrel.gov/docs/fy17osti/68214.pdf>.
- Tangerås, T.P. and J. Mauritzen (2018), “Real-Time versus Day-Ahead Market Power in a Hydro-Based Electricity Market,” *J. Ind. Econ.*, 66(4): 904–941.
- Tejada-Arango, D.A., S. Wogrin, and E. Centeno (2018), “Representation of Storage Operations in Network-Constrained Optimization Models for Medium- and Long-Term Operation,” *IEEE Trans. Power Syst.*, 33(1): 386–396.
- Virasjoki, V., P. Rocha, A.S. Siddiqui, and A. Salo (2016), “Market Impacts of Energy Storage in a Transmission-Constrained Power System,” *IEEE Trans. Power Syst.*, 31: 4108–4117.
- Virasjoki, V., A.S. Siddiqui, B. Zakeri, and A. Salo (2018), “Market Power with Combined Heat and Power Production in the Nordic Energy System,” *IEEE Trans. Power Syst.*, 33: 5263–5275.
- Wong, B., A. Sumner, and P. Ludewig (2009), *Pumped Storage Powers Up for New York Summer*, <http://www.waterpowermagazine.com/features/featurepumped-storage-powers-up-for-new-york-summer/>.